representing bilateral SII activities. PLV between two channels was calculated as follows:

$$PLV^{m,n}(t,f_0) = \left| \frac{1}{N} \sum_{k=1}^{N} \frac{\Phi_k^m(t,f_0)}{|\Phi_k^m(t,f_0)|} / \frac{\Phi_k^n(t,f_0)}{|\Phi_k^n(t,f_0)|} \right|$$

where m and n denote channels comprising the reference sensor and target sensor, respectively. PLV was calculated for each single trial, and the PLVs of 100 trials were averaged in each subject. PLVs are shown as an index ranging from 0 to 1.

Third, we examined phase-locking statistics (PLS) to determine whether the calculated PLVs were significantly correlated with the stimuli. PLS was defined by the proportion of surrogate PLVs higher than the original PLVs. The surrogate PLV represents the PLV calculated between signals of different trials:

$$PLV^{m,n}_{surrogate}(t,f_0) = \left| \frac{1}{100} \sum_{k=1}^{100} \frac{\Phi^m_{\mathrm{perm}(k)}(t,f_0)}{|\Phi^m_{\mathrm{perm}(k)}(t,f_0)|} / \frac{\Phi_k^n(t,f_0)}{|\Phi_k^n(t,f_0)|} \right|$$

Here, we calculated the surrogate PLVs from 200 different permutations of trials. The statistically significant PLV was defined as the presence of surrogated PLVs of less than 10 trials larger than original PLVs (that is, PLS<0.05). Furthermore, the mean PLV of the pre-stimulus period (−100 to 0 ms) was subtracted from the PLV of the

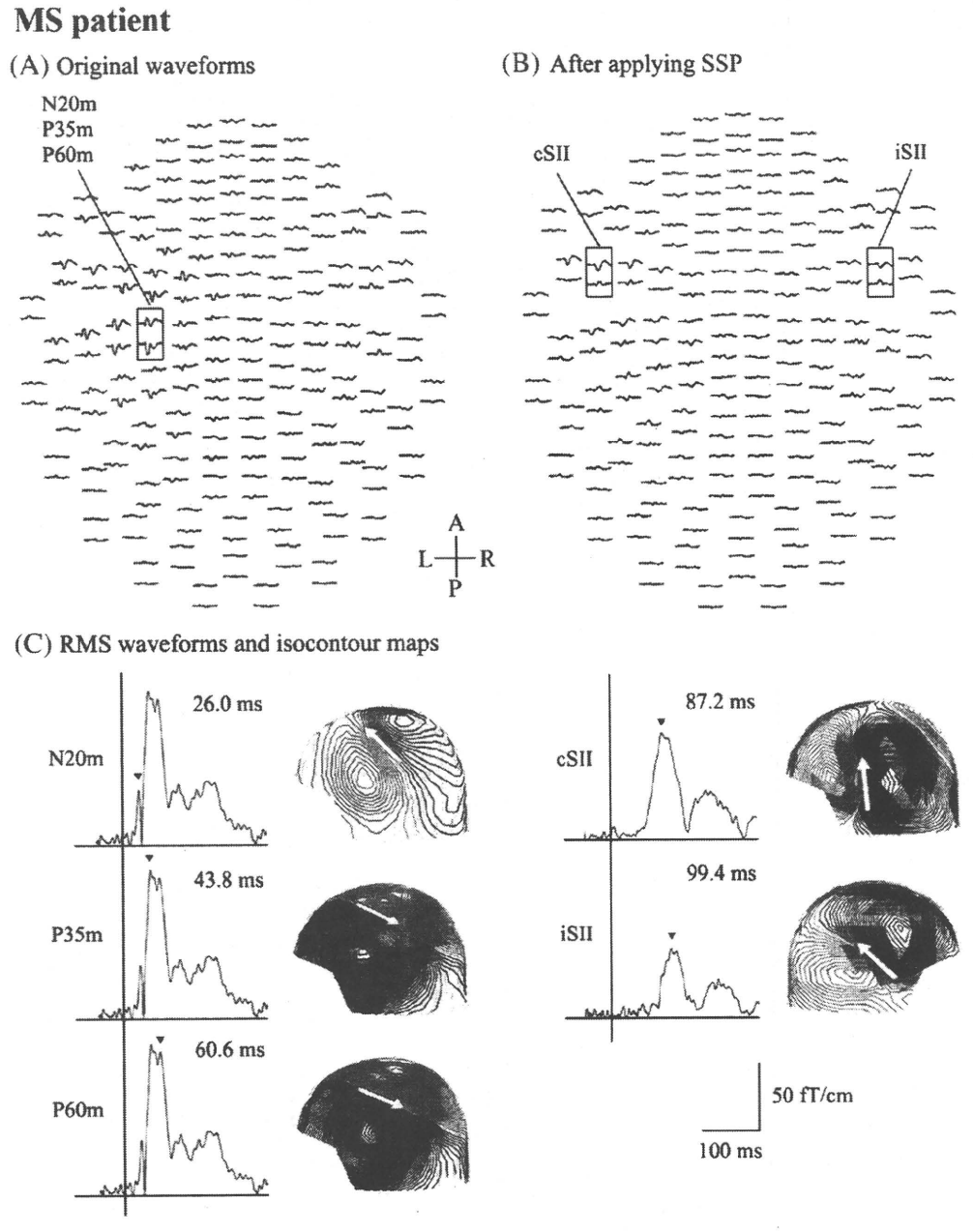

Fig. 2. Analysis of SEFs in an MS patient. The latencies of all cSI deflections (namely, N20m, P35m, and P60m) are prolonged compared with those in the normal subjects, whereas bilateral SII responses are evoked with comparable latencies. The amplitude of the N20m deflection is decreased, but other deflections, including the bilateral SII, are comparable in the amplitude to those in normal subjects.

Table 1
Latencies and amplitudes (mean ± SD) of the RMS waveforms.

	Latency (ms)			Amplitude (fT/cm)		
	Normal	MS	p value	Normal	MS	p value
N20m	21.4 ± 1.0 (n = 46)	23.5 ± 3.8 (n = 45)	0.027*	64.9 ± 30.1	52.1 ± 25.9	0.018*
P35m	32.0 ± 5.0 (n = 46)	35.6 ± 6.5 (n = 40)	0.005*	75.3 ± 48.7	74.3 ± 39.1	0.616
P60m	53.8 ± 7.6 (n = 46)	57.8 ± 8.4 (n = 46)	0.01*	90.2 ± 31.3	88.2 ± 47.4	0.281
cSII	91.2 ± 15.8 (n = 46)	87.2 ± 14.9 (n = 46)	0.153	60.8 ± 23.4	65.0 ± 33.6	0.656
iSII	104.2 ± 19.8 (n = 44)	104.1 ± 22.9 (n = 41)	0.728	41.4 ± 18.0	41.9 ± 18.6	0.778

* P<0.05: when compared with the values in normal subjects using the Mann–Whitney U-test.

post-stimulus period; thus, only event-related phase synchronization of gamma-band activities was evaluated.

For the analysis of the group average, we selected regions of interest (ROIs) as follows: the frequency range was 30–70 Hz, and the latency period was 0–200 ms. PLVs were calculated for each orthogonally oriented pair of channels to minimize crosstalk noise, and the mean PLV was calculated from the ROI in each subject. Only PLVs with larger means were accepted for the group-averaged PLV (p<0.05 by Rayleigh test).

Results

SEFs of SI and SII

In line with the results of previous studies (Kakigi, 1994; Wikström et al., 1996; Lin and Forss, 2002; Huttunen et al., 2006), we recorded five major deflections of the SEF waveforms in the cSI and bilateral SII areas. Figs. 1 and 2 show the representative SEF waveforms and isocontour maps obtained from normal subjects and MS patients. Short-latency deflections, N20m, P35m, and P60m, which corresponded to the activities of the cSI area, were identified over the contralateral centro-parietal area. Middle-latency deflections were observed over the bilateral temporo-parietal area with the deflection contralateral to the stimulation peaking earlier than the deflection ipsilateral to the stimulation: the former corresponds to the activity of cSII, while the latter corresponds to the activity of iSII. All cSI deflections were clearly identified in all normal subjects, whereas N20m and P35m deflections were not recorded in one hemisphere (p = 0.31) and six hemispheres (p<0.01), respectively, in MS patients. The cSII deflection was identified in all normal subjects as well as in all MS patients. The iSII deflection was undetectable in two hemispheres in normal subjects and in five hemispheres in MS patients (p = 0.22).

Regarding the side-to-side difference within each group, there were no significant differences in the peak latencies or in the amplitudes between the left and right median nerves. Therefore, the data for left and right median nerve stimulations were combined for the statistical analysis. Table 1 shows the latencies and amplitudes of the RMS waveforms. The mean latencies of all of the cSI deflections were significantly prolonged in MS patients (p<0.05). By contrast, there were no significant differences in the latencies of bilateral SII deflections. In both groups, cSII and iSII were recorded at around 90 and 100 ms after stimulation, respectively. The mean amplitudes of the N20m deflection were significantly smaller in MS patients (p<0.05). The amplitudes of other deflections showed no significant differences between MS and normal subjects. No significant correlation was found between the latencies for N20m and cSII in both

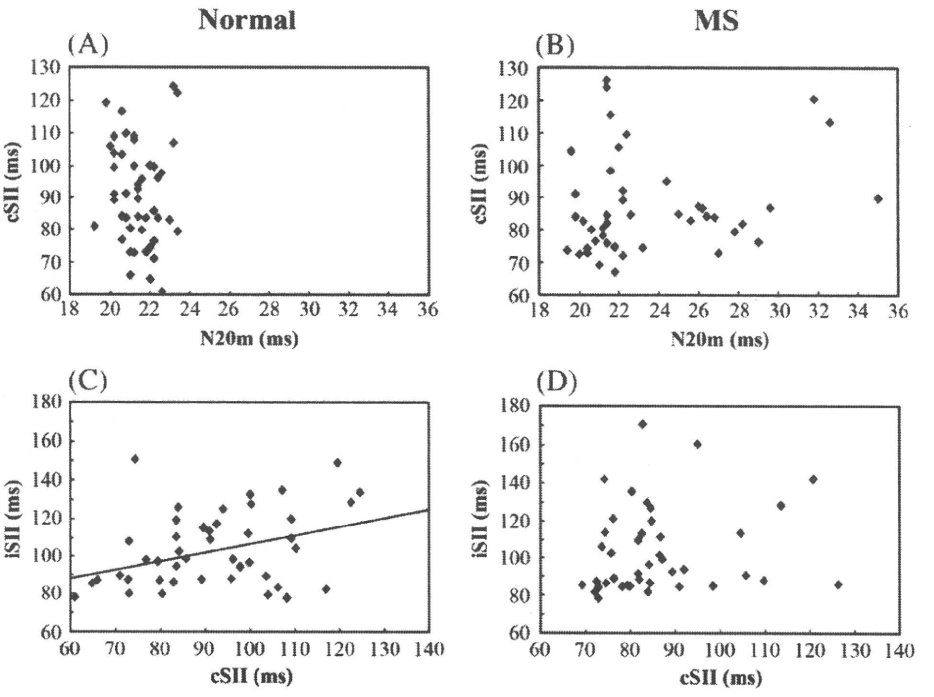

Fig. 3. A linear regression analysis of correlation between the latencies of cSI and cSII shows no significant correlation both in normal subjects (A; r = 0.09, p = 0.55) and MS patients (B; r = 0.18, p = 0.23). Correlation analysis between the latencies of cSII and iSII shows a significant correlation in normal subjects (C; r = 0.361, p = 0.016) but not in MS patients (D; r = 0.158, p = 0.323).

groups (Fig. 3A and B). There was a significant correlation between the latencies of cSII and iSII in normal subjects ($p<0.05$) (Fig. 3C), but no correlation was found in MS patients (Fig. 3D). The mean locations and strengths of the ECDs for each deflection were almost comparable with those reported previously (see Supplemental data) (Wikström et al., 1996; Wegner et al., 2000; Kida et al., 2006). Fig. 4 shows the locations of the ECDs superimposed on the MRI in representative subjects of both groups, demonstrating that the ECDs are located in the appropriate cortices (i.e., SI and SII).

PLVs between SI and SII

The temporal-frequency analysis with the continuous wavelet transformation showed the induced gamma-band activities both in the SI and SII areas (Figs. 5 and 6). They started at early post-stimulus period and continued up to 200 ms. In normal subjects, high-frequency gamma activities (50–70 Hz) were observed in cSI, and to a lesser degree in cSII. Low-frequency gamma activities (30–40 Hz) were distributed in all three areas (i.e., cSI, cSII, and iSII). Interestingly, the power of the high-frequency gamma activities (50–70 Hz) was relatively reduced in MS patients. Figs. 7 and 8 show the grand averaged PLVs in the gamma-band (30–70 Hz) for the normal subjects and MS patients. Overall, PLVs were calculated in the range of 0–0.15. In normal subjects, significantly increased PLVs between cSI and cSII were observed mostly within the time window 0–100 ms after the stimulus onset (Fig. 7A). Increased PLVs in the higher frequency gamma-band (50–70 Hz) were observed within the early period (0–50 ms) following the stimulus onset, whereas high PLVs in the lower frequency gamma-band (30–40 Hz) tended to last for a longer period, up to 100 ms. In addition, there were some weak but statistically significant PLVs of various frequency bands in the later time window 100–200 ms. On the contrary, the cSI–cSII phase synchrony was significantly decreased in MS patients, both in the high-frequency gamma-band (50–70 Hz) and the low-frequency gamma-band (30–40 Hz) (Fig. 7B). The degree of decrease in the PLVs between cSI and cSII was most prominent around 40 Hz. Regarding the phase synchrony between the cSII and iSII areas, significantly increased PLVs in the low-frequency gamma-band (30–40 Hz) were observed during the time interval 30–100 ms in normal subjects (Fig. 8A), whereas such an increase in PLVs was diminished in MS patients (Fig. 8B).

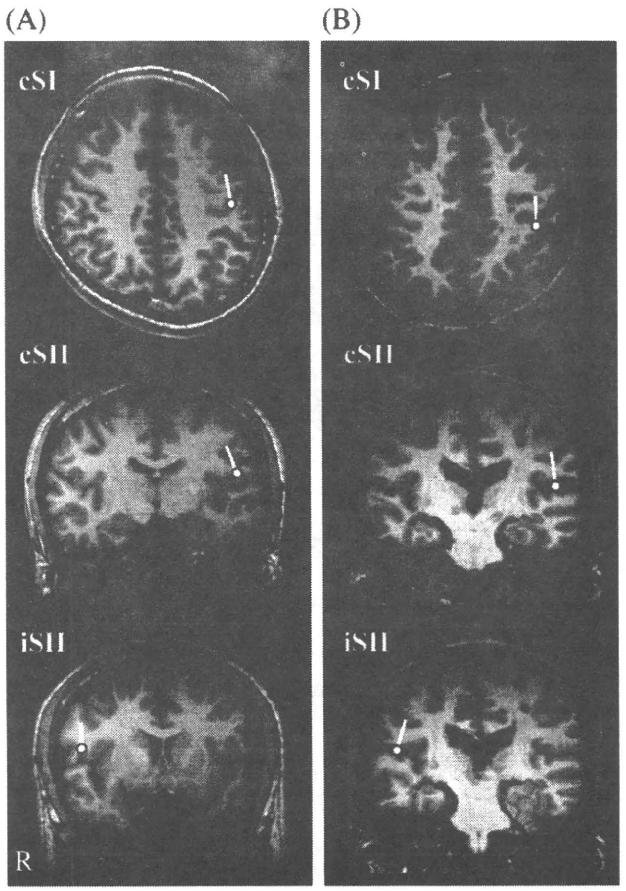

Fig. 4. ECD locations in a normal subject (A) and an MS patient (B) superimposed on MRI. For this view, cSI (N20m) and bilateral SII sources are located in the appropriate cortices in both subjects. The MS patient has scattered small hypointensities in the periventricular and juxtacortical white matter.

Discussion

Neuronal synchronization in the gamma-frequency band has received increasing attention as the salient mechanism for cortico-cortical information processing (Tallon-Baudry and Bertrand, 1999; Engel and Singer, 2001; Buzsáki and Draguhn, 2004; Knight, 2007; Womelsdorf et al., 2007). Recently, the temporal binding mechanism in various gamma-frequency bands has been well recognized in several studies of top–down and bottom–up information processing among anatomically distributed cortical areas (Tallon-Baudry et al., 1997; Engel et al., 2001; Womelsdorf et al., 2006; Buschman and Miller, 2007; Saalmann et al., 2007). However, the significance of temporal binding theory in the functional relationship between SI and SII has not yet been established. In this study, we assessed the temporal binding mechanism by PLVs of induced gamma activity, and our results provided evidence for functional interaction in the early somatosensory processing. To our knowledge, we first demonstrated that synchronized gamma-band activities in both between cSI and cSII and between cSII and iSII occurred in the early post-stimulus stage. Therefore, the oscillatory gamma synchronization binds the early-stage tactile information processing within the somatosensory cortical network.

Previous studies demonstrated that broadband oscillatory activities including the gamma-frequency bands were present and enhanced in relation to the attentive task in the early-stage somatosensory processing areas (Palva et al., 2005; Bauer et al., 2006). Until recently, no studies have examined the gamma-band phase synchronization between the SI and SII areas. Only cSI–iSII phase-locking in the alpha- and beta-frequency bands has been demonstrated in healthy subjects (Simões et al., 2003). Therefore, our study is the first to demonstrate the early-latency neural synchrony within the gamma-band between SI and SII, which may well represent the parallel mode of the early-stage tactile somatosensory processing. Although we did not perform attentive task to enhance the oscillatory gamma activity, the increase in PLVs after the stimulus onset (see Fig. 7) may be associated with ongoing cortical activities facilitating the later stages of somatosensory processing and perceptual process (Palva et al., 2005).

It is well known that SII receives direct thalamocortical projections from several nuclei of the thalamus, including the ventroposterior lateral nucleus, the ventroposterior inferior nucleus, the ventroposterior medial nucleus, the central lateral nucleus, and the posterior nucleus (Friedman and Murray, 1986; Krubitzer and Kaas, 1992; Stevens et al., 1993). In a study that applied a cortical cooling procedure in marmoset monkeys (Zhang et al., 1996, 2001), evoked responses and responsiveness of individual neurons in SII were rarely abolished by inactivation of SI, and the study claimed that SI and SII occupied a hierarchically equivalent position in the somatosensory system. In humans, simultaneous activation of SI and SII was suggested by an MEG study (Karhu and Tesche, 1999), which demonstrated very early evoked responses of SII; the initial activity

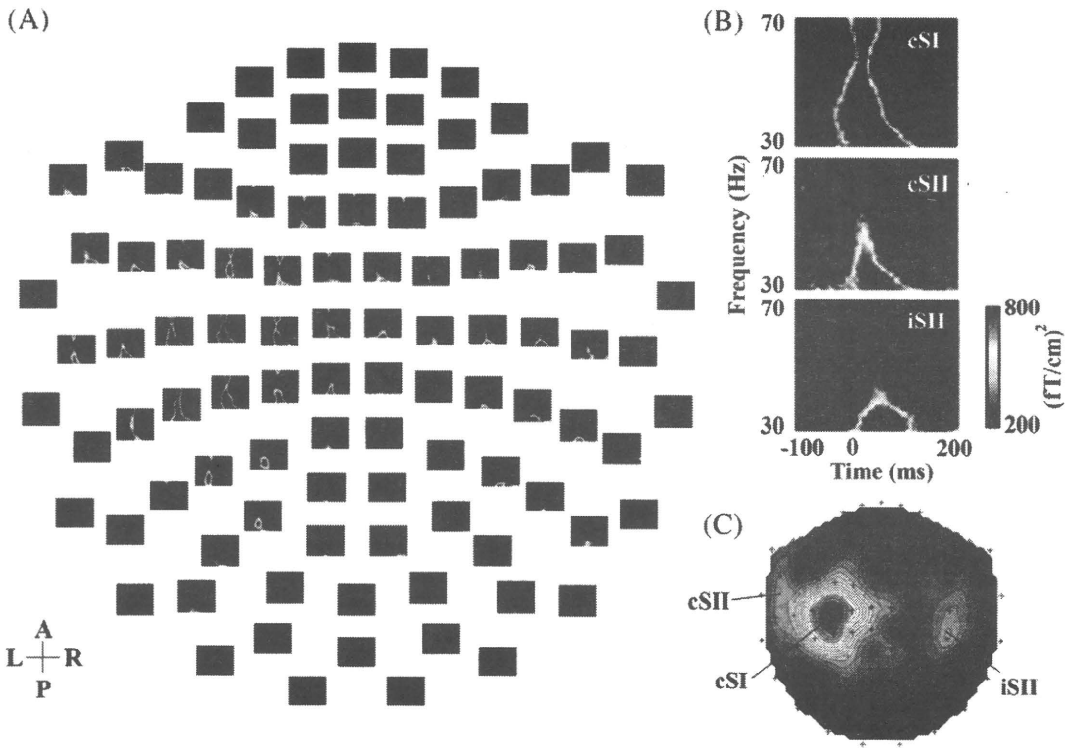

Fig. 5. (A) Temporal-frequency analysis for all gradiometer sensors in a representative normal subject. (B) Induced gamma-band activities (30–70 Hz) recorded by the sensors showing the SI and SII activities. (C) Topography of the induced gamma activities around the SI and SII areas.

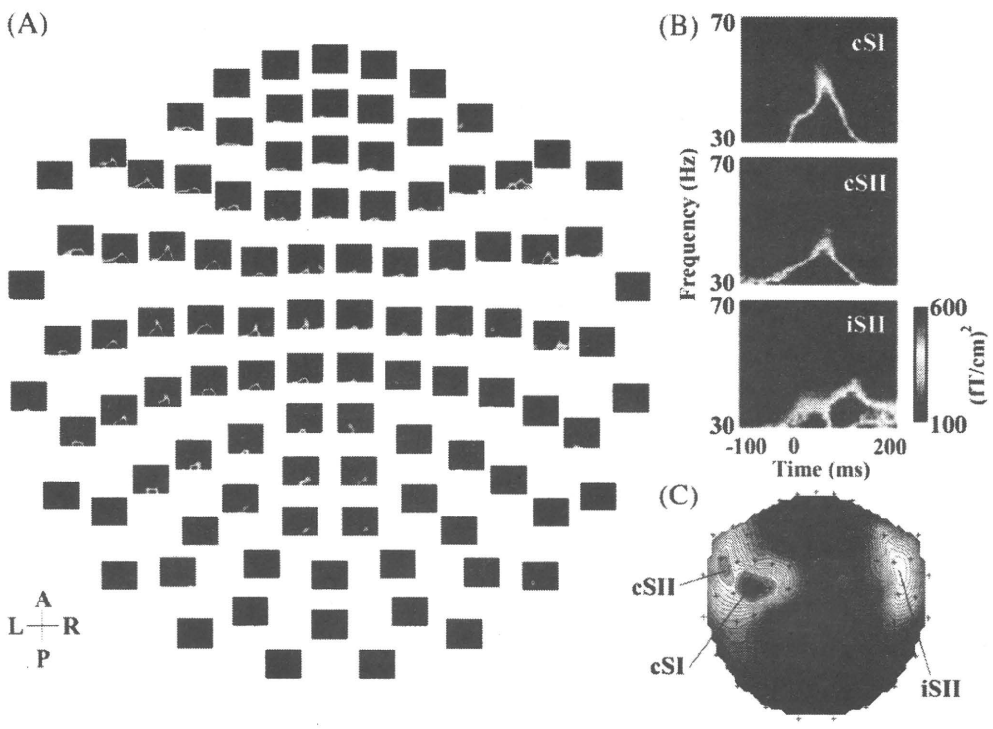

Fig. 6. (A) Temporal-frequency analysis for all gradiometer sensors in a representative MS patient. (B) Induced gamma activities recorded by the sensors showing the SI and SII activities. In contrast to normal subjects, the absolute power of the high-frequency gamma activities (50–70 Hz) is relatively reduced in cSI. (C) Topography of the induced gamma activities around the SI and SII areas.

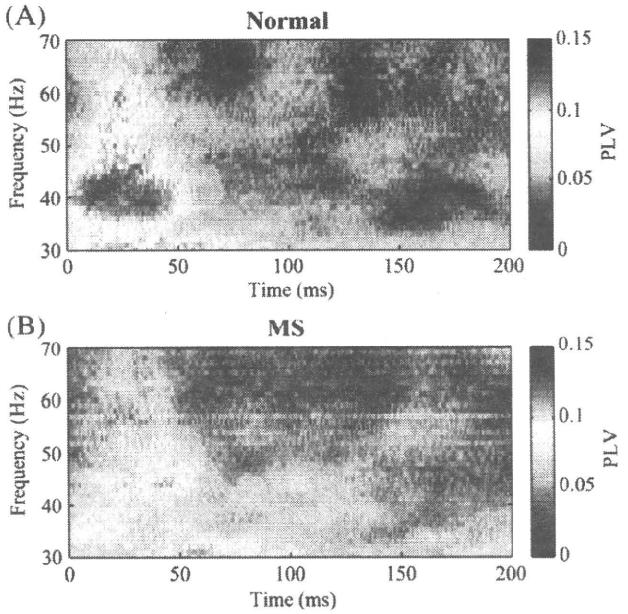

Fig. 7. Analysis of PLVs between cSI and cSII. (A) The grand average of PLVs in normal subjects shows increased PLVs in the entire gamma-frequency band (30–70 Hz). The high PLVs in the high-frequency gamma-band (50–70 Hz) are observed in the earlier latencies (mostly in the post-stimulus period of 20–50 ms), whereas those in the low-frequency gamma-band (30–40 Hz) last up to 100 ms. There are also some phase-locking activities of various frequencies during the later post-stimulus period (>100 ms). (B) In MS patients, decreased PLVs are noted in the entire frequency range.

of cSII started at around 20 ms after electrical stimulation of the median nerve, consistent with the latency of the direct thalamocortical conduction to SII. Likewise, short-latency responses in SII were reported by a study with direct cortical recording (Barba et al., 2002), which demonstrated that SEPs in SII could be generated at around 30 ms after the median nerve stimulation. Furthermore, transcranial magnetic stimulation delivered at the SII area at about 20 ms after electrical stimulation of the median nerve specifically caused facilitatory effect on motor reaction time (Raij et al., 2008), which proposed the presence of the direct thalamocortical pathway to SII. Although we could not record the early-latency evoked responses in SII, our results revealed a nonlinear relationship between the evoked responses in SI and SII. There was no significant correlation between the latencies of N20m and cSII both in normal subjects and MS patients. Moreover, analysis of SEFs showed no significant differences in the latencies and amplitudes of SII responses despite the prolonged latencies and decreased amplitudes of cSI deflections in MS patients. Thus, it is plausible that the early-latency gamma oscillations in SII, as reflected by the increased PLVs, might be partly mediated by the direct thalamocortical input to SII.

We demonstrated the decrease in PLVs between SI and SII in MS patients compared with normal control subjects. The temporal-frequency analysis demonstrated the preserved low-frequency gamma activities (30–40 Hz) in MS patients, whereas the phase synchronization was significantly impaired in the corresponding frequency range. We also found that the PLVs between cSI and cSII were reduced in the high-frequency gamma-band (50–70 Hz), while the power of the high-gamma activities was relatively decreased. One may argue that the decreased PLVs in the high-frequency gamma-band may be attributable to the reduced power of the activity in MS patients. However, PLV is theoretically independent of the power fluctuations (Lachaux et al., 1999). Because subcortical U-fiber lesions and periventricular white matter lesions in MS patients may frequently involve the intra- and interhemispheric associative pathways, the lesion load might significantly contribute to the decreased neuronal synchronization within the somatosensory cortical network. In accord with this view, the significance of such altered functional connectivity in MS patients was reported by some studies (Leocani et al., 2000; Cover et al., 2006; Arrondo et al., 2009), demonstrating disturbed neuronal synchrony in various frequency bands. The impaired interhemispheric functional connectivity in MS was also suggested by the non-correlation between the cSII and iSII latencies in the patient group. Although the assessment of intracortical connectivity within SI in MS patients has been performed by a recent MEG study using a synchronization index for the gamma-band activity (Tecchio et al., 2008), it is notable that this is the first MEG study to demonstrate impaired functional connectivity between SI and SII in MS.

Our study also raises a question regarding the general assumption that cSII and iSII are activated sequentially via the transcallosal fibers. We observed no significant difference in the latencies and amplitudes of iSII between the healthy subjects and MS patients, despite the altered cSI activity and the impairment of functional connectivity between cSII and iSII in the latter group. Our findings suggest that the functional disconnection of the bilateral somatosensory cortices does not have a significant impact on iSII activity. Similarly, a previous MEG study performed in patients with ischemic stroke lesions showed preserved responses of iSII, despite the diminished responses of cSI and cSII (Forss et al., 1999). These observations suggest that iSII receives direct input from the thalamus, and thus, the responsiveness of iSII is relatively independent of the activities of the contralateral somatosensory cortices.

The multifocality of the lesions in MS may be a methodological reservation of this study. The effect of individual lesions could not be simply weighed due to dissemination of the lesions in the CNS. In addition, we observed no significant changes in the evoked responses of SII despite the impaired SI response in MS. One may argue that thalamocortical inputs can be reduced both in SI and SII and that the SII activities could also be affected. Since our patients showed only mild disability, patients with more severe disability may reveal different characteristics on the SII responses. Alternatively, given that

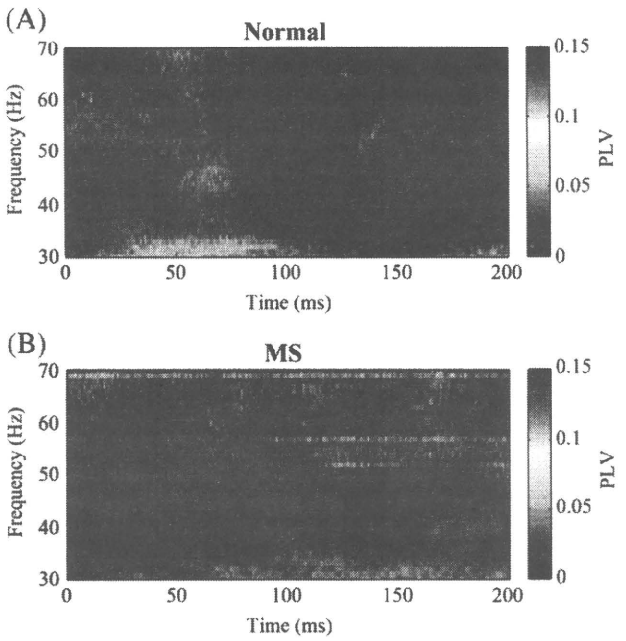

Fig. 8. Analysis of PLVs between cSII and iSII. (A) The grand average of PLVs in normal subjects shows significantly increased PLVs in the low-frequency gamma-band (30–40 Hz), which occurs between 30 and 100 ms. (B) Such an increase in PLVs is barely noticeable in MS patients.

SI receives input exclusively from the VPL and SII receives inputs from the multiple nuclei in the thalamus, it seems convincing that there exists a nonlinear relationship between the SI and SII responses. In accord with our assumption, an fMRI study demonstrated that patients with a solitary infarction of the VPL showed preserved activity of SII despite the reduced activation of SI (Taskin et al., 2006).

In conclusion, the analysis of PLVs demonstrated early neuronal synchronization between SI and SII. The decrease of PLVs in MS validated the significance of increased PLVs in healthy subjects. The current study provides evidence for the gamma-band synchrony in the early-stage human somatosensory processing.

Acknowledgment

This study was supported in part by a Grant-in-aid for Scientists, No 19390242, from the Ministry of Education, Culture, Sports, Science and Technology in Japan.

Appendix A. Supplementary data

Supplementary data associated with this article can be found, in the online version, at doi:10.1016/j.neuroimage.2010.02.001.

References

Arrondo, G., Alegre, M., Sepulcre, J., Iriarte, J., Artieda, J., Villoslada, P., 2009. Abnormalities in brain synchronization are correlated with cognitive impairment in multiple sclerosis. Mult. Scler. 15, 509–516.
Balzamo, E., Marquis, P., Chauvel, P., Régis, J., 2004. Short-latency components of evoked potentials to median nerve stimulation recorded by intracerebral electrodes in the human pre- and postcentral areas. Clin. Neurophysiol. 115, 1616–1623.
Barba, C., Frot, M., Mauguière, F., 2002. Early secondary somatosensory area (SII) SEPs. Data from intracerebral recordings in humans. Clin. Neurophysiol. 113, 1778–1786.
Barkhof, F., Filippi, M., Miller, D.H., Scheltens, P., Campi, A., Polman, C.H., Comi, G., Ader, H.J., Losseff, N., Valk, J., 1997. Comparison of MRI criteria at first presentation to predict conversion to clinically definite multiple sclerosis. Brain 120, 2059–2069.
Bauer, M., Oostenveld, R., Peeters, M., Fries, P., 2006. Tactile spatial attention enhances gamma-band activity in somatosensory cortex and reduces low-frequency activity in parieto-occipital areas. J. Neurosci. 26, 490–501.
Buschman, T.J., Miller, E.K., 2007. Top-down versus bottom-up control of attention in the prefrontal and posterior parietal cortices. Science 315, 1860–1862.
Buzsáki, G., Draguhn, A., 2004. Neuronal oscillations in cortical networks. Science 304, 1926–1929.
Calabrese, P., Penner, I.K., 2007. Cognitive dysfunctions in multiple sclerosis—a "multiple disconnection syndrome"? J. Neurol. 254 (Suppl. 2), II18–II21.
Cover, K.S., Vrenken, H., Geurts, J.J., van Oosten, B.W., Jelles, B., Polman, C.H., Stam, C.J., van Dijk, B.W., 2006. Multiple sclerosis patients show a highly significant decrease in alpha band interhemispheric synchronization measured using MEG. Neuroimage 29, 783–788.
Dineen, R.A., Vilisaar, J., Hlinka, J., Bradshaw, C.M., Morgan, P.S., Constantinescu, C.S., Auer, D.P., 2009. Disconnection as a mechanism for cognitive dysfunction in multiple sclerosis. Brain 132, 239–249.
Engel, A.K., Singer, W., 2001. Temporal binding and the neural correlates of sensory awareness. Trends Cogn. Sci. 5, 16–25.
Engel, A.K., Fries, P., Singer, W., 2001. Dynamic predictions: oscillations and synchrony in top-down processing. Nat. Rev. Neurosci. 2, 704–716.
Forss, N., Hari, R., Salmelin, R., Ahonen, A., Hämäläinen, M., Kajola, M., Knuutila, J., Simola, J., 1994. Activation of the human posterior parietal cortex by median nerve stimulation. Exp. Brain Res. 99, 309–315.
Forss, N., Merlet, I., Vanni, S., Hämäläinen, M., Mauguière, F., Hari, R., 1996. Activation of human mesial cortex during somatosensory target detection task. Brain Res. 734, 229–235.
Forss, N., Hietanen, M., Salonen, O., Hari, R., 1999. Modified activation of somatosensory cortical network in patients with right-hemisphere stroke. Brain 122, 1889–1899.
Friedman, D.P., Murray, E.A., 1986. Thalamic connectivity of the second somatosensory area and neighboring somatosensory fields of the lateral sulcus of the macaque. J. Comp. Neurol. 252, 348–373.
Frot, M., Mauguière, F., 1999. Timing and spatial distribution of somatosensory responses recorded in the upper bank of the sylvian fissure (SII area) in humans. Cereb. Cortex 9, 854–863.
He, Y., Dagher, A., Chen, Z., Charil, A., Zijdenbos, A., Worsley, K., Evans, A., 2009. Impaired small-world efficiency in structural cortical networks in multiple sclerosis associated with white matter lesion load. Brain 132, 3366–3379.
Huttunen, J., Komssi, S., Lauronen, L., 2006. Spatial dynamics of population activities at S1 after median and ulnar nerve stimulation revisited: an MEG study. Neuroimage 32, 1024–1031.
Inui, K., Wang, X., Tamura, Y., Kaneoke, Y., Kakigi, R., 2004. Serial processing in the human somatosensory system. Cereb. Cortex 14, 851–857.
Iwamura, Y., 1998. Hierarchical somatosensory processing. Curr. Opin. Neurobiol. 8, 522–528.
Kakigi, R., 1994. Somatosensory evoked magnetic fields following median nerve stimulation. Neurosci. Res. 20, 165–174.
Karhu, J., Tesche, C.D., 1999. Simultaneous early processing of sensory input in human primary (SI) and secondary (SII) somatosensory cortices. J. Neurophysiol. 81, 2017–2025.
Kida, T., Wasaka, T., Inui, K., Akatsuka, K., Nakata, H., Kakigi, R., 2006. Centrifugal regulation of human cortical responses to a task-relevant somatosensory signal triggering voluntary movement. Neuroimage 32, 1355–1364.
Knight, R.T., 2007. Neuroscience. Neural networks debunk phrenology. Science 316, 1578–1579.
Krubitzer, L.A., Kaas, J.H., 1992. The somatosensory thalamus of monkeys: cortical connections and a redefinition of nuclei in marmosets. J. Comp. Neurol. 319, 123–140.
Kurtzke, J.F., 1983. Rating neurologic impairment in multiple sclerosis: an expanded disability status scale (EDSS). Neurology 33, 1444–1452.
Lachaux, J.P., Rodriguez, E., Martinerie, J., Varela, F.J., 1999. Measuring phase synchrony in brain signals. Hum. Brain Mapp. 8, 194–208.
Leocani, L., Locatelli, T., Martinelli, V., Rovaris, M., Falautano, M., Filippi, M., Magnani, G., Comi, G., 2000. Electroencephalographic coherence analysis in multiple sclerosis: correlation with clinical, neuropsychological, and MRI findings. J. Neurol. Neurosurg. Psychiatry 69, 192–198.
Lin, Y.Y., Forss, N., 2002. Functional characterization of human second somatosensory cortex by magnetoencephalography. Behav. Brain Res. 135, 141–145.
Matsuoka, T., Matsushita, T., Kawano, Y., Osoegawa, M., Ochi, H., Ishizu, T., Minohara, M., Kikuchi, H., Mihara, F., Ohyagi, Y., Kira, J., 2007. Heterogeneity of aquaporin-4 autoimmunity and spinal cord lesions in multiple sclerosis in Japanese. Brain 130, 1206–1223.
Mauguière, F., Merlet, I., Forss, N., Vanni, S., Jousmäki, V., Adeleine, P., Hari, R., 1997. Activation of a distributed somatosensory cortical network in the human brain. A dipole modelling study of magnetic fields evoked by median nerve stimulation. Part I: location and activation timing of SEF sources. Electroencephalogr. Clin. Neurophysiol. 104, 281–289.
Palva, S., Linkenkaer-Hansen, K., Näätänen, R., Palva, J.M., 2005. Early neural correlates of conscious somatosensory perception. J. Neurosci. 25, 5248–5258.
Polman, C.H., Reingold, S.C., Edan, G., Filippi, M., Hartung, H.P., Kappos, L., Lublin, F.D., Metz, L.M., McFarland, H.F., O'Connor, P.W., Sandberg-Wollheim, M., Thompson, A.J., Weinshenker, B.G., Wolinsky, J.S., 2005. Diagnostic criteria for multiple sclerosis: 2005 revisions to the "McDonald Criteria". Ann. Neurol. 58, 840–846.
Pons, T.P., Garraghty, P.E., Friedman, D.P., Mishkin, M., 1987. Physiological evidence for serial processing in somatosensory cortex. Science 237, 417–420.
Raij, T., Karhu, J., Kičić, D., Lioumis, P., Julkunen, P., Lin, F.H., Ahveninen, J., Ilmoniemi, R.J., Mäkelä, J.P., Hämäläinen, M., Rosen, B.R., Belliveau, J.W., 2008. Parallel input makes the brain run faster. Neuroimage 40, 1792–1797.
Saalmann, Y.B., Pigarev, I.N., Vidyasagar, T.R., 2007. Neural mechanisms of visual attention: how top-down feedback highlights relevant locations. Science 316, 1612–1615.
Simões, C., Jensen, O., Parkkonen, L., Hari, R., 2003. Phase locking between human primary and secondary somatosensory cortices. Proc. Natl. Acad. Sci. U. S. A. 100, 2691–2694.
Stevens, R.T., London, S.M., Apkarian, A.V., 1993. Spinothalamocortical projections to the secondary somatosensory cortex (SII) in squirrel monkey. Brain Res. 631, 241–246.
Tallon-Baudry, C., Bertrand, O., 1999. Oscillatory gamma activity in humans and its role in object representation. Trends Cogn. Sci. 3, 151–162.
Tallon-Baudry, C., Bertrand, O., Delpuech, C., Permier, J., 1997. Oscillatory gamma-band (30–70 Hz) activity induced by a visual search task in humans. J. Neurosci. 17, 722–734.
Taskin, B., Jungehulsing, G.J., Ruben, J., Brunecker, P., Krause, T., Blankenburg, F., Villringer, A., 2006. Preserved responsiveness of secondary somatosensory cortex in patients with thalamic stroke. Cereb. Cortex 16, 1431–1439.
Taulu, S., Simola, J., 2006. Spatiotemporal signal space separation method for rejecting nearby interference in MEG measurements. Phys. Med. Biol. 51, 1759–1768.
Tecchio, F., Zito, G., Zappasodi, F., Dell'Acqua, M.L., Landi, D., Nardo, D., Lupoi, D., Rossini, P.M., Filippi, M.M., 2008. Intra-cortical connectivity in multiple sclerosis: a neurophysiological approach. Brain 131, 1783–1792.
Wegner, K., Forss, N., Salenius, S., 2000. Characteristics of the human contra- versus ipsilateral SII cortex. Clin. Neurophysiol. 111, 894–900.
Wikström, H., Huttunen, J., Korvenoja, A., Virtanen, J., Salonen, O., Aronen, H., Ilmoniemi, R.J., 1996. Effects of interstimulus interval on somatosensory evoked magnetic fields (SEFs): a hypothesis concerning SEF generation at the primary sensorimotor cortex. Electroencephalogr. Clin. Neurophysiol. 100, 479–487.
Womelsdorf, T., Fries, P., Mitra, P.P., Desimone, R., 2006. Gamma-band synchronization in visual cortex predicts speed of change detection. Nature 439, 733–736.
Womelsdorf, T., Schoffelen, J.M., Oostenveld, R., Singer, W., Desimone, R., Engel, A.K., Fries, P., 2007. Modulation of neuronal interactions through neuronal synchronization. Science 316, 1609–1612.
Zhang, H.Q., Murray, G.M., Turman, A.B., Mackie, P.D., Coleman, G.T., Rowe, M.J., 1996. Parallel processing in cerebral cortex of the marmoset monkey: effect of reversible SI inactivation on tactile responses in SII. J. Neurophysiol. 76, 3633–3655.
Zhang, H.Q., Zachariah, M.K., Coleman, G.T., Rowe, M.J., 2001. Hierarchical equivalence of somatosensory areas I and II for tactile processing in the cerebral cortex of the marmoset monkey. J. Neurophysiol. 85, 1823–1835.

Journal of Neurochemistry

JNC

JOURNAL OF NEUROCHEMISTRY | 2011 | 116 | 828–832 doi: 10.1111/j.1471-4159.2010.07020.x

MINI-REVIEW

Antibodies against ganglioside complexes in Guillain-Barré syndrome and related disorders

Susumu Kusunoki* and Ken-ichi Kaida†

*Department of Neurology, Kinki University School of Medicine, Osaka, Japan

†Third Department of Internal Medicine, National Defense Medical College, Saitama, Japan

Abstract

Guillain-Barré syndrome (GBS) is acute autoimmune neuropathy, often subsequent to an infection. Serum anti-ganglioside antibodies are frequently elevated in titer. Those antibodies are useful diagnostic markers and possible pathogenetic factors. Recent data demonstrated that sera from some patients with GBS react with ganglioside complexes (GSCs) consisting of two different gangliosides, but not with each constituent ganglioside. Those antibodies may specifically recognize a new conformational epitope formed by two gangliosides. In particular, the antibodies against GD1a/GD1b and/or GD1b/GT1b complexes are associated with severe GBS requiring artificial ventilation. The antibodies to GM1/GalNAc–GD1a and those to GSCs containing GQ1b or GT1a are associated with pure motor GBS and Fisher syndrome, respectively. In contrast, the binding activities of the antibodies highly specific to GD1b are strongly inhibited by the addition of GD1a to GD1b. Gangliosides along with other components as cholesterol are known to form lipid rafts, in which two different gangliosides may form a new conformational epitope. Future investigation is necessary to elucidate the roles of GSCs in the plasma membrane and of the clinical relevance of the anti-GSCs antibodies.

Keywords: ganglioside, Guillain-Barré syndrome, membrane microdomain, peripheral nerve.

J. Neurochem. (2011) **116**, 828–832.

Anti-ganglioside antibodies, mostly IgG type, are present in the sera from approximately 60% of patients with Guillain-Barré syndrome (GBS), acute immune-mediated polyradiculoneuropathy (Willison and Yuki 2002; Kusunoki *et al.* 2008; Van Doorn *et al.* 2008). Because the presence of anti-ganglioside antibodies in the acute-phase sera is a characteristic feature of GBS, those antibodies can be used as diagnostic markers of GBS. There are many molecular species of gangliosides, named depending on the carbohydrate sequences. Each ganglioside has unique distribution within the PNS. Considering the gangliosides are localized in the plasma membrane with their carbohydrate portions extended to the extracellular spaces, the anti-ganglioside antibodies may function in the pathogenesis of GBS through antibody-antigen interaction in PNS.

IgG anti-GQ1b antibody is one of the best studied antibodies. Ig anti-GQ1b antibodies are specifically associated with a variant of GBS, Fisher syndrome (FS) characterized by ophthalmoplegia and ataxia (Chiba *et al.* 1992). Anti-GQ1b monoclonal antibody specifically immunostains paranodal myelin of human cranial nerves innervating extraocular muscles (Chiba *et al.* 1993) and some large neurons in dorsal root ganglia (Kusunoki *et al.* 1999). It has recently been reported that the neuromuscular junctions of human extraocular muscles are richly bound by the antibodies against GQ1b and GT1a (Liu *et al.* 2009). Thus, the anti-GQ1b antibodies may cause opthalmoplegia and ataxia by binding to the regions where GQ1b is densely localized.

Measurement of anti-ganglioside antibodies has been conducted with ELISA or TLC-immunostaining by the use of purified single ganglioside antigens. Gagliosides have characteristics of forming clusters in the plasma membrane

Received July 27, 2010; revised manuscript received September 26, 2010; accepted September 28, 2010.

Address correspondence and reprint requests to Susumu Kusunoki, 377-2 Ohno-Higashi, Osaka-Sayama, Osaka 589-8511, Japan.
E-mail: kusunoki-tky@umin.ac.jp

Abbreviations used: AMCBN, acute motor conduction block neuropathy; FS, Fisher syndrome; GBS, Guillain-Barré syndrome; GSC, ganglioside complex; LOS, lipooligosaccharides.

(Hakomori 2002). In the clusters, the carbohydrate structure of a ganglioside may interact with each other to form a novel epitope. We recently demonstrated that some GBS patients had serum antibodies that specifically recognize the novel glycoepitopes formed by two individual ganglioside molecules and named such antibodies as 'anti-ganglioside complex (GSC) antibodies' (Kaida *et al.* 2004).

Antibodies to ganglioside complexes in GBS

Antibodies to GD1a/GD1b and GD1b/GT1b complexes in severe GBS

Anti-GD1a/GD1b complex antibodies are the first identified antibodies against GSCs. We investigated a serum from a GBS patient who showed acute severe flaccid tetraparesis and needed artificial ventilation. We found an unidentified immuno-reactive band in the position just below GD1a on TLC of a crude ganglioside fraction from bovine brain. The serum was not reactive with any of such purified gangliosides as GM1, GM2, GM3, GD1a, GD1b, GD3, GalNAc–GD1a, GT1b, and GQ1b. But the serum IgG bound strongly to the well coated with the mixture of GD1a and GD1b gangliosides (GD1a/GD1b complex). When GD1a and GD1b were developed in the same lane on TLC using a developing solvent, chloroform/methanol/0.2%$CaCl_2 \cdot 2H_2O$ (50 : 45 : 10), the serum IgG strongly immunostained just the overlapping portion between GD1a and GD1b. When another developing solvent (C/M/0.2%$CaCl_2 \cdot 2H_2O$, 30/65/10) that completely separated the positions of GD1a and GD1b was used, no immunoreaction was identified. Those data indicate that mixing GD1a and GD1b may produce a new conformational glycoepitope which is different from that of GD1a or GD1b alone and the antibody in sera from the above patient may specifically recognize such a new glycoepitope.

We next investigated antibodies in sera from 234 GBS patients with ELISA using a mixture of two of the four major gangliosides (GM1, GD1a, GD1b and GT1b) (Kaida *et al.* 2007). The sera with anti-GSC antibodies often exhibited to some extent reactivity with constituent gangliosides of the GSCs. When optical density for the anti-GD1a/GD1b antibody was 0.2 higher than that corresponding to anti-GD1a or anti-GD1b antibody or it was more than the sum of those of anti-GD1a and anti-GD1b antibodies, the sera were judged to be anti-GD1a/GD1b-positive. The same criteria also were applied to the other GSCs. The cutoff value (0.2) for anti-GSC antibodies was decided arbitrarily. The results showed that 39 of 234 patients (17%) had antibodies against at least one of the mixture antigens. All the 39 patients had anti-GM1/GD1a antibodies, 27 had anti-GM1/GT1b antibodies, 16 had anti-GD1a/GD1b antibodies, and 13 had GD1b/GT1b antibodies. Most of anti-GD1a/GD1b or anti-GD1b/GT1b antibody reacted also with GM1/GT1b as well as GM1/GD1a. Immunoabsorption study suggested that anti-GSC antibodies specifically react with clustered glycoepitopes common to these GSCs, rather than individually with each GSC. An epitope formed by a combination of [Galβ1-3GalNAc] and [NeuAcα2-3Galβ1-3GalNAc] in the terminal moieties of ganglio-*N*-tetraose structures is likely to be essential for the antibody binding. Among them, antibodies against GD1a/GD1b and GD1b/GT1b complexes were significantly associated with severe GBS requiring artificial ventilation (Kaida *et al.* 2007). Those antibodies can be useful markers of severe GBS. Future study is needed to clarify why anti-GD1a/GD1b and GD1b/GT1b antibodies are associated with severe disabilities.

Antibodies to ganglioside complexes including GQ1b

Because FS is considered to be a variant of GBS, we extended an investigation of anti-GSC antibodies to FS patients. Presence of anti-ganglioside complexes antibodies in FS therefore was investigated with ELISA using seven ganglioside antigens; GM1, GM2, GD1a, GD1b, GT1a, GT1b and GQ1b (Kaida *et al.* 2006).

Acute phase serum samples were collected from 12 FS patients, 10 of whom had IgG anti-GQ1b antibodies. ELISA results showed that seven patients had antibodies to GSCs such as GQ1b/GM1, GQ1b/GD1b, GQ1b/GD1a, GQ1b/GT1b, GT1a/GM1, GT1a/GD1b, and GT1a/GD1a, but not to the complexes without GQ1b and GT1a. One patient had no anti-GQ1b or anti-GT1a antibodies, but had antibodies to GQ1b/GM1 and GT1a/GM1. Specific immunoreactivities against the overlapping portion of the two gangliosides were confirmed by TLC-immunostaining. In contrast to GBS, no FS patients had antibodies to the complexes consisting of two of the four major gangliosides, GM1, GD1a, GD1b and GT1b.

The results of anti-GSCs antibody assay on larger number of patients with FS and those with GBS with opthalmoplegia indicated that the serum antibodies could be subdivided into the three groups (Kanzaki *et al.* 2008): (i) antibodies specific to GQ1b and/or GT1a without anti-GSCs reactivity; (ii) antibodies that recognize a combination of [Galβ1-3GalNAc] and [NeuAcα2-8 NeuAcα2-3Galβ1-3GalNAc] in the terminal residues of ganglio-*N*-tetraose structures, such as antibodies to GQ1b/GM1, GQ1b/GD1b, GT1a/GM1, GT1a/GD1b (Fig. 1); and (iii) antibodies that recognize a combination of [NeuAcα2-3Galβ1-3GalNAc] and [NeuAcα2-8 NeuAcα2-3Galβ1-3GalNAc] in the terminal residues, such as antibodies to GQ1b/GD1a, GT1a/GD1a, GQ1b/GT1b, GT1a /GT1b. In addition, recent report showed that some patients have the antibodies specific to GQ1b/GA1 (Ogawa *et al.* 2009).

Sensory signs were infrequent in FS patients with antibodies to GQ1b/GM1 but were frequent in patients with other types of antibodies. However, the clinical relevance of such anti-GSC antibodies needs to be investigated in future.

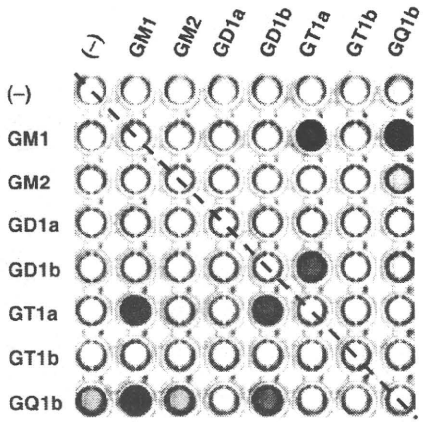

Fig. 1 An ELISA plate showing the binding activities of a serum antibody that recognizes a combination of [Galβ1-3GalNAc] and [NeuAcα2-8NeuAcα2-3 Galβ1-3GalNAc] in the terminal residues. All the wells in each line and column were coated with a respective ganglioside (e.g. the wells in the first line and column were coated only with a single ganglioside, the well in the eighth line and the second column was coated with GQ1b and GM1), except for those on the oblique dotted line that were uncoated control wells. The antibody binds strongly to GQ1b/GM1, GQ1b/GD1b, GT1a/GM1 and GT1a/GD1b but only weakly to GQ1b.

Antibodies to GM1/GalNAc–GD1a complex in pure motor GBS

IgG antibodies against GM1 or those against GalNAc–GD1a are known to closely correlate with acute motor axonal neuropathy (Kaida *et al.* 2000; Willison and Yuki 2002). We investigated antibody activities against the mixture of GM1 and GalNAc–GD1a (GM1/GalNAc–GD1a complex) in a large population of patients with GBS. The results showed that ten of 224 GBS patients had IgG antibodies to the GM1/GalNAc–GD1a complex (Kaida *et al.* 2008a).

We then analyzed the clinical and electrophysiologic findings of those 10 anti-GM1/GalNAc–GD1a-positive patients. Respiratory infections preceded the neurological onset in six cases and gastrointestinal infections in two cases. Therefore, although *Campylobacter jejuni* is an infectious agent that frequently causes the antecedent infection of GBS cases with anti-GM1 and anti-GalNAc–GD1a antibodies, *C. jejuni* may not be the major infectious agent inducing anti-GM1/GalNAc–GD1a complex antibodies. Cranial nerve involvement and sensory signs are infrequent. Early motor conduction block at intermediate nerve segments was found in five patients. Generally, the response to therapy was good. According to the criteria established by Hadden *et al.* (1998), four were categorized as demyelinative and two were axonal. When judged by other criteria (Ho *et al.* 1995), four were demyelinative and three were axonal.

Table 1 Representative anti-GSCs antibodies in GBS and FS

Antigen	Associated disease	Frequency (%)	Clinical features
GD1a/GD1b	GBS	7	Severe GBS
GD1b/GT1b	GBS	6	Severe GBS
GM1/GalNAc–GD1a	GBS	4	Pure motor GBS AMCBN
GQ1b/GM1 and related GSCs	FS	41	Infrequent sensory dysfunction
	GBS with OP	28	
GQ1b/GD1a and related GSCs	FS	6	
	GBS with OP	19	

GSC, ganglioside complex; GBS, Guillain-Barré syndrome; FS, Fisher syndrome; AMCBN, acute motor conduction block neuropathy; OP, ophthalmoplegia.
GQ1b/GM1 and related GSCs, GQ1b/GM1, GQ1b/GD1b, GT1a/GM1, GT1a/GD1b; GQ1b/GD1a and related GSCs, GQ1b/GD1a, GT1a/GD1a, GQ1b/GT1b, GT1a /GT1b.

The clinical findings of the 10 GBS patients were consistent with a pure motor variant of GBS. Clinical features of anti-GM1/GalNAc–GD1a IgG-positive GBS resemble those of acute motor conduction block neuropathy (AMCBN), in view of preserved sensory function, early conduction block at intermediate nerve segments and good recovery (Capasso *et al.* 2003). IgG anti-GM1 antibody (and sometimes anti-GalNAc–GD1a antibody) was reported in their sera. However, IgG anti-GM1 or anti-GalNAc–GD1a antibodies are frequently detected in sera of acute motor axonal neuropathy type GBS and conduction block is not common in such cases. Anti-GM1/GalNAc–GD1a antibody is likely to cause early reversible changes on the axolemma and may be more closely associated with AMCBN than the anti-GM1 or anti-GalNAc–GD1a antibody. GM1 and GalNAc–GD1a may form a complex in the axolemma at nodes of Ranvier or paranodes of the motor nerves, and may be a target antigen in pure motor GBS; especially in the form of AMCBN.

Representative anti-GSCs antibodies in GBS and FS are listed in the Table 1.

Antibodies against ganglioside complexes in chronic neuropathies

Nobile-Orazio *et al.* (2010) investigated serum IgM antibodies to GSCs in such chronic neuropathies as multifocal motor neuropathy, chronic inflammatory demyelinating polyradiculoneuropathy and IgM paraproteinemic neuropathy. As a result, one of 34 chronic inflammatory demyelinating polyradiculoneuropathy patients had IgM antibody activity to GT1b/GM1 and GT1b/GM2, and one of 23 IgM paraproteinemic neuropathy patients had IgM anti-GM2/GD1b activity.

Production of antibodies against ganglioside complexes

In GBS and related disorders subsequent to *C. jejuni* infection, anti-ganglioside antibodies are shown to be induced by the immune reaction against lipo-oligosaccharides (LOS) of pathogens causing antecedent infection (Willison and Yuki 2002; Van Doorn *et al.* 2008). A similar mechanism can be speculated in the production of anti-GSC antibodies. Kuijf *et al.* (2007) recently reported that such anti-GSC antibodies as anti-GM1/GD1a and GQ1b/GD1a cross-reacted to LOS from the autologous *C. jejuni* strain, indirectly demonstrating that the LOS contained GSC-like structures. However, carbohydrate structures expressed in the LOS may not exactly be the combination of the two carbohydrate chains expected from the reactivity of the serum anti-GSC antibodies.

Inhibition of the reactivity of the anti-ganglioside antibody by another coexistent ganglioside

If the interaction of two gangliosides creates a new epitope with conformational changes, the binding acitivity of the antibody highly specific to one ganglioside may be lessened by the addition of another ganglioside to make an antigen mixture.

We investigated sera from 17 GBS patients who had IgG antibody reactive only with GD1b in routine antibody assay. For those sera, antibody activity against a mixture of GD1b and another ganglioside was examined and compared the activity with that against GD1b alone. The results showed that the addition of GD1a, GT1a, GT1b, GQ1b and GalNAc–GD1a to GD1b caused marked decrease of the binding activity of anti-GD1b antibodies, suggesting that those gangliosides may interact with GD1b to make a novel epitope which cannot be easily recognized by the anti-GD1b antibodies (Kaida *et al.* 2008b).

In addition, the reduction rates of the binding activities caused by the addition of such gangliosides as GD1a, GT1b, GQ1b and GalNAc–GD1a were significantly more in the antibodies from ataxic patients than in those from non-ataxic patients. The addition of another ganglioside may cause conformational change. Therefore, the more specific the antibody is, the more affected its reactivity should be. It therefore suggests that the anti-GD1b IgG antibodies in ataxic patients may be more specific to GD1b than those in patients without ataxia. This may provide further evidence to the association between anti-GD1b antibody and ataxia (Kusunoki *et al.* 1996).

Thus, the antibodies specific to GD1a/GD1b complex are associated with severe GBS (Fig. 2) and those specific to GD1b itself are associated with the development of ataxia (Fig. 3).

A similar inhibitory effect of neighboring gangliosides has recently been reported in the case of anti-GM1 antibodies by

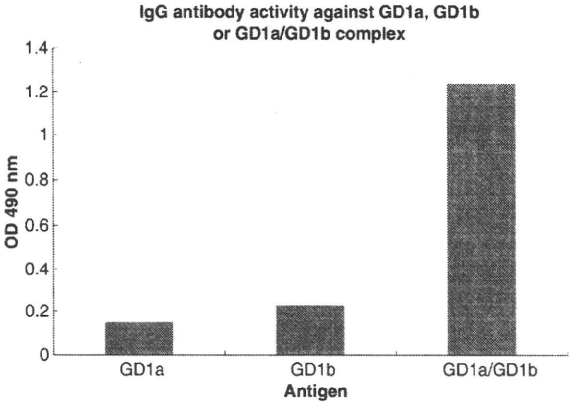

Fig. 2 ELISA result on a serum sample from a patient with severe Guillain-Barré syndrome (Kaida *et al.* 2004). This patient's serum IgG shows strong reaction with a mixture of GD1a and GD1b (GD1a/GD1b) but reacts only weakly with GD1a or GD1b alone.

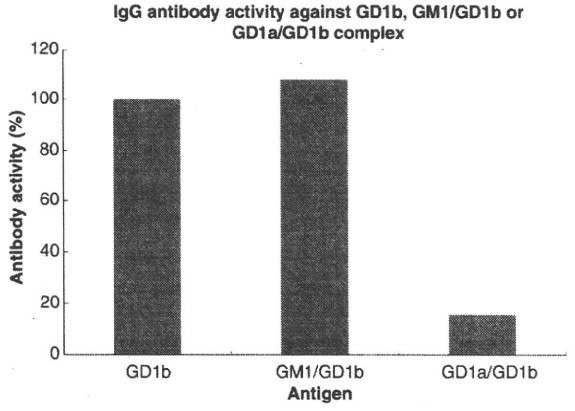

Fig. 3 The IgG antibody activities to mixture antigens in sera from nine GBS patients with ataxia who had only IgG anti-GD1b antibody in routine antibody assay (Kaida *et al.* 2008b). Bars of GM1/GD1b and GD1a/GD1b showed the average activities of the nine patients. Compared with the antibody activity to GD1b alone (100%), the activity was markedly reduced because of the addition of GD1a to GD1b antigen whereas the addition of GM1 did not affect the antibody activity.

Greenshields *et al.* (2009). Negative effects by gangalioside complexes on the binding of IgM anti-GM1 antibodies in sera from patients with chronic immune-mediated neuropathies, particularly multifocal motor neuropathy, have also been reported (Nobile-Orazio *et al.* 2010).

Future studies on the anti-GSC antibodies in the pathogenesis of autoimmune neuropathies

Gangliosides are located in the cell membranes with carbohydrate portions on the outer surfaces, and are preferentially

packaged with cholesterol, forming lipid rafts. Within rafts, gangliosides are considered to interact with important transmembrane receptors or signal transducers (Simons and Ikonen 1997; Hakomori 2002). Anti-GSC antibodies may cause dysfunction of the axon or Schwann cells through their binding to clustered epitopes of glycosphingolipids in the plasma membrane microdomains. Future study on the localization of each ganglioside complex is needed. Animal model of the autoimmune neuropathy mediated by anti-GSC antibodies should also be developed. Such investigations may lead to the understanding of the roles of GSCs in the plasma membrane and of the clinical relevance of the anti-GSCs antibodies.

Acknowledgements

This work was supported by the Ministry of Education, Culture, Sports, Science and Technology of Japan (Grants-in-Aid for Scientific Research, 21390273) and the Ministry of Health Labour, and Welfare of Japan (Health and Labour Sciences Research Grants for Research on intractable diseases (Neuroimmunological Diseases) (H20-016) and for Comprehensive Research on Disability Health and Welfare, H21-012).

References

Capasso M., Caporale C. M., Pomilio F., Gandolfi P., Lugaresi A. and Uncini A. (2003) Acute motor conduction block neuropathy: another Guillain-Barré syndrome variant. *Neurology* **61**, 617–622.

Chiba A., Kusunoki S., Shimizu T. and Kanazawa I. (1992) Serum IgG antibody to gangalioside GQ1b is a possible marker of Miller Fisher syndrome. *Ann. Neurol.* **31**, 677–679.

Chiba A., Kusunoki S., Otaba H., Machinami R. and Kanazawa I. (1993) Serum anti-GQ1b IgG antibody is associated with ophthalmoplegia in Miller Fisher syndrome and Guillain-Barré syndrome: clinical and immunohistochemical studies. *Neurology* **43**, 1911–1917.

Greenshields K. N., Halstead S. K., Zitman F. M. *et al.* (2009) The neuropathic potential of anti-GM1 autoantibodies is required by the local glycolipid environment in mice. *J. Clin. Invest.* **119**, 595–610.

Hadden R. D. M., Cornblath D. R., Hughes R. A., Zielasek J., Hartung H. P., Toyka K. V. and Swan A. V. (1998) Electrophysiological classification of Guillain-Barré syndrome: clinical associations and outcome: Plasma Exchange/Sandoglobulin Guillain-Barré Syndrome Trial Group. *Ann. Neurol.* **44**, 780–788.

Hakomori S. (2002) The glycosynapse. *Proc. Natl Acad. Sci. USA* **99**, 225–232.

Ho T. W., Mishu B., Li C. Y., Gao C. Y., Cornblath D. R., Griffin J. W., Asbury A. K., Blaser M. J. and McKhann G. M. (1995) Guillain-Barré syndrome in northern China. Relationship to *Campylobacter jejuni* infection and anti-glycolipid antibodies. *Brain* **118**, 597–605.

Kaida K., Kusunoki S., Kamakura K., Motoyoshi K. and Kanazawa I. (2000) Guillain-Barré syndrome with antibody to a ganglioside, *N*-acctylgalactosaminyl GD1a. *Brain* **123**, 116–124.

Kaida K., Morita D., Kanzaki M., Kamakura K., Motoyoshi K., Hirakawa M. and Kusunoki S. (2004) Ganglioside complexes as new target antigens in Guillain-Barré syndrome. *Ann. Neurol.* **56**, 567–571.

Kaida K., Kanzaki M., Morita D., Kamakura K., Motoyoshi K., Hirakawa M. and Kusunoki S. (2006) Anti-ganglioside complex antibodies in Miller Fisher syndrome. *J. Neurol. Neurosurg. Psychiatry* **77**, 1043–1046.

Kaida K., Morita D., Kanzaki M., Kamakura K., Motoyoshi K., Hirakawa M. and Kusunoki S. (2007) Anti-ganglioside complex antibodies associated with severe disability in GBS. *J. Neuroimmunol.* **182**, 212–218.

Kaida K., Sonoo M., Ogawa G., Kamakura K., Ueda-Sada M., Arita M., Motoyoshi K. and Kusunoki S. (2008a) GM1/GalNAc–GD1a complex: a target for pure motor Guillain-Barré syndrome. *Neurology* **71**, 1683–1690.

Kaida K., Kamakura K., Ogawa G., Ueda M., Motoyoshi K., Arita M. and Kusunoki S. (2008b) GD1b-specific antibody induces ataxia in Guillain-Barré syndrome. *Neurology* **71**, 196–201.

Kanzaki M., Kaida K., Ueda M., Morita D., Hirakawa M., Motoyoshi K., Kamakura K. and Kusunoki S. (2008) Ganglioside complexes containing GQ1b as targets in Miller Fisher and Guillain-Barre syndrome. *J. Neurol. Neurosurg. Psychiatry* **79**, 1148–1152.

Kuijf M. L., Godschalk P. C., Gilbert M., Endtz H. P., Tio-Gillen A. P., Ang C. W., van Doorn P. A. and Jacobs B. C. (2007) Origin of ganglioside complex antibodies in Guillain-Barré syndrome. *J. Neuroimmunol.* **188**, 69–73.

Kusunoki S., Shimizu J., Chiba A., Ugawa Y., Hitoshi S. and Kanazawa I. (1996) Experimental sensory neuropathy induced by sensitization with ganglioside GD1b. *Ann. Neurol.* **39**, 424–431.

Kusunoki S., Chiba A. and Kanazawa I. (1999) Anti-GQ1b IgG antibody is associated with ataxia as well as ophthalmoplegia. *Muscle Nerve* **22**, 1071–1074.

Kusunoki S., Kaida K. and Ueda M. (2008) Antibodies against gangliosides and ganglioside complexes in Guillain-Barré syndrome: new aspects of research. *Biochim. Biophys. Acta* **1780**, 441–444.

Liu J.-X., Willison H. J. and Pedrosa-Domellof F. (2009) Immunolocalization of GQ1b and related gangliosides in human extraocular neuromuscular junctions and muscle spindles. *Invest. Ophthalmol. Vis. Sci.* **50**, 3226–3232.

Nobile-Orazio E., Giannotta C. and Briani C. (2010) Anti-ganglioside complex IgM antibodies in multifocal motor neuropathy and chronic immune-mediated neuropathies. *J. Neuroimmunol.* **219**, 119–122.

Ogawa G., Kaida K., Kusunoki S., Ueda M., Kimura F. and Kamakura K. (2009) Antibodies to ganglioside complexes consisting of asialo-GM1 and GQ1b or GT1a in Fisher and Guillain-Barre syndromes. *J. Neuroimmunol.* **214**, 125–127.

Simons K. and Ikonen E. (1997) Functional rafts in cell membranes. *Nature* **387**, 569–572.

Van Doorn P., Ruts L. and Jacobs B. (2008) Clinical features, pathogenesis, and treatment of Guillain-Barré syndrome. *Lancet Neurol.* **7**, 939–950.

Willison H. J. and Yuki N. (2002) Peripheral neuropathies and anti-glycolipid antibodies. *Brain* **125**, 2591–2625.

Clinica Chimica Acta 411 (2010) 1774–1780

Contents lists available at ScienceDirect

Clinica Chimica Acta

journal homepage: www.elsevier.com/locate/clinchim

Comparison of low-density lipoprotein cholesterol concentrations measured by a direct homogeneous assay and by the Friedewald formula in a large community population

Kozo Tanno [a,*], Tomonori Okamura [b], Masaki Ohsawa [a], Toshiyuki Onoda [a], Kazuyoshi Itai [a], Kiyomi Sakata [a], Motoyuki Nakamura [c], Akira Ogawa [d], Kazuko Kawamura [e], Akira Okayama [f]

[a] Department of Hygiene and Preventive Medicine, School of Medicine, Iwate Medical University, Morioka, Japan
[b] Division of Preventive Cardiology, National Cerebral and Cardiovascular Center, Osaka, Japan
[c] Division of Cardiology, Department of Internal Medicine, School of Medicine, Iwate Medical University, Morioka, Japan
[d] Department of Neurosurgery, School of Medicine, Iwate Medical University, Japan
[e] Iwate Health Service Association, Morioka, Japan
[f] The First Institute of Health Service, Japan Anti-Tuberculosis Association, Tokyo, Japan

ARTICLE INFO

Article history:
Received 16 March 2010
Received in revised form 26 July 2010
Accepted 26 July 2010
Available online 3 August 2010

Keywords:
Low-density lipoprotein cholesterol
Enzymatic homogeneous LDL-C assay
Friedewald formula
Triglyceride
Japanese
Community-based study

ABSTRACT

Background: We compare the direct homogeneous low-density lipoprotein cholesterol (LDL-C) assay with the Friedewald formula (FF) for determination of LDL-C in a large community-dwelling population.
Methods: A total of 21,194 apparently healthy subjects aged 40 to 79 years with triglyceride (TG) concentrations <4.52 mmol/l were enrolled. LDL-C were directly measured by the enzymatic homogeneous assay (LDL-C (D)) and also estimated by the FF (LDL-C (F)). Paired t-test, Pearson's correlation coefficient and linear regression analysis were performed and the concordances of the National Cholesterol Education Program (NCEP) risk category were estimated.
Results: Both in fasting (n = 3270) and nonfasting samples (n = 17,924), LDL-C (D) highly correlated with LDL-C (F): $r = 0.971$ and 0.955, respectively. Concordant results for NCEP categories were 84.8% for fasting samples and 80.1% for nonfasting samples. However, the bias between the 2 measurements increased in samples with TG concentrations >1.69 mmol/l, especially in nonfasting samples.
Conclusions: The results showing less variability of the direct LDL-C assay than that of the FF in nonfasting samples suggest that epidemiological studies can use LDL-C measured by the direct assay both in fasting and nonfasting samples.

1. Introduction

Many epidemiological studies and clinical trials have shown that elevated low-density lipoprotein cholesterol (LDL-C) concentrations are causally related to an increased risk of coronary artery disease (CAD) [1,2]. The findings from those studies are mainly based on LDL-C concentrations calculated by the Friedewald formula (LDL-C (F)) [3], which derives LDL-C concentrations from total cholesterol (TC), high-density lipoprotein cholesterol (HDL-C) and triglyceride (TG) concentrations [4–7]. The guidelines for preventing atherosclerotic disease recommend using the Friedewald formula in a fasting state (ideally a 9- to 12-h fast) [1,2]. However, it is impossible to obtain fasting samples from all patients who visit clinics, especially those who visit at night or in the afternoon. In Japan, general screenings for risk factors of cardiovascular disease (CVD) are performed under nonfasting conditions to improve the participation rates. Therefore, a convenient method for determination of LDL-C concentration that is insensitive to postprandial state has been required regardless of whether it is directly obtained or calculated.

Recently, several homogeneous assays have been used as direct measurements for determination of LDL-C concentration. They have become popular in clinics and in health check-ups. Most homogeneous assays have met the National Cholesterol Education Program (NCEP) total error goals for nondiseased individuals in a fasting state compared with β-quantification [8,9]. In addition, no significant difference in LDL-C concentrations measured by the direct homogeneous assay was seen

Abbreviations: LDL-C, low-density lipoprotein cholesterol; TG, triglyceride; LDL-C (F), LDL-C calculated by the Friedewald formula; LDL-C (D), LDL-C measured by the enzymatic homogeneous assay; CAD, coronary artery disease; TC, total cholesterol; HDL-C, high-density lipoprotein cholesterol; CVD, cardiovascular disease; NCEP, National Cholesterol Education Program; CRMLN, Cholesterol Reference Method Laboratory Network; HbA1c, glycosylated hemoglobin; SBP, systolic blood pressure; DBP, diastolic blood pressure; BMI, body mass index; NCEP-ATP III, National Cholesterol Education Program Adult Treatment Panels III; OR, odds ratio; CI, confidence interval.

* Corresponding author. Department of Hygiene and Preventive Medicine, School of Medicine, Iwate Medical University, 19-1 Uchimaru, Morioka, Iwate 020-8505, Japan. Tel.: +81 19 651 5111x3373; fax: +81 19 623 8870.
E-mail address: ktanno@iwate-med.ac.jp (K. Tanno).

0009-8981/$ – see front matter © 2010 Elsevier B.V. All rights reserved.
doi:10.1016/j.cca.2010.07.034

between paired fasting and nonfasting samples in the same individuals [10,11], and postprandial changes in LDL-C concentrations measured by the homogeneous assay were similar to those measured by β-quantification [12].

On the other hand, the Friedewald formula is known to underestimate LDL-C concentrations compared with β-quantification even when TG concentrations are <4.52 mmol/l [13–15]. The calculated LDL-C concentrations also have been reported to be significantly decreased in a postprandial state [16–18]. However, in recent large-scale population-based cohort studies, CVD risk has been assessed using LDL-C concentrations calculated by the Friedewald formula in a nonfasting state because of a strong correlation between LDL-C concentrations obtained by the Friedewald formula and β-quantification [19,20] and there are only minimal changes in concentrations of LDL-C in response to normal food intake in a general population [21]. These studies suggest that LDL-C concentrations calculated by the Friedewald formula either in fasting or nonfasting samples could be used in population-based epidemiological studies.

We therefore compared the direct homogeneous LDL-C assay with the Friedewald formula for determination of LDL-C both in fasting and nonfasting samples using baseline data from a large cohort study of community-dwelling residents to clarify whether the direct homogeneous LDL-C assay can be used in population-based epidemiological studies.

2. Materials and methods

2.1. Study population

We analyzed baseline data of the Iwate-Kenpoku cohort (Iwate-KENCO) study, which was designed as a cohort study of community-dwelling residents living in the northern part of the main island of Japan. The methodology of the Iwate-KENCO study was described elsewhere [22–24]. The baseline survey was carried out between 2002 and 2005. Of 24,572 participants (8476 men and 16,096 women) aged 40 to 79 years from whom we obtained written informed consent for participation in this study, 594 subjects with missing data for serum lipids, 212 subjects with TG concentrations >4.52 mmol/l (400 mg/dl) and 54 subjects who did not have complete information were excluded from the analysis. Furthermore, 1697 subjects receiving medication for dyslipidemia and 821 subjects with a history of stroke or myocardial infarction were excluded to examine whether LDL-C concentrations measured by the direct homogeneous assay can be used as baseline data in an epidemiological study assessing the risk of first CVD events in the general community-dwelling population. Therefore, 21,194 participants (7349 men and 13,845 women) were enrolled in the present study. The study was approved by the Medical Ethics Committee of Iwate Medical University and conducted in accordance with the guidelines of the Declaration of Helsinki.

2.2. Measurements of serum lipids

Samples from participants whose last meal was ≥12 h before their blood draw were used as fasting samples (n = 3270) and samples from participants who had eaten within 12 h of their blood draw were used as nonfasting samples (n = 17,924). Both fasting and nonfasting samples were collected into vacuum tubes containing a serum separator gel. The samples were stored immediately after sampling in an icebox and were transported to a laboratory (Iwate Health Service Association) and analyzed on the same day. Serum TC, TG and HDL-C concentrations were measured by an enzymatic method. Serum LDL-C concentrations were measured by an enzymatic homogenous assay with Cholestest-LDL (Daiichi Chemicals, currently Sekisui Medical, Tokyo). LDL-C was also estimated again using the Friedewald formula. Non-HDL-C was calculated by subtracting HDL-C from TC. Measurements for TC, HDL-C and LDL-C (homogenous assay), except for the TG assay, have been standardized by the Osaka Medical Center for Health Science and Promotion, a member of the Cholesterol Reference Method Laboratory Network (CRMLN) controlled by the Centers for Disease Control and Prevention (Atlanta, USA) [25] and have met all criteria for both precision and accuracy of lipid measurement. During the period of the baseline survey, total coefficient of variations (CVs), mean biases and total errors for LDL-C assay used in this study were 0.2% to 0.4%, 0.7% to 0.8% and 1.2% to 1.5%, respectively. The corresponding values for the TC assay were −2.7% to 0.4%, 0.2% to 0.4% and 1.2% to 3.5%, and the corresponding values for the HDL-C assay were −2.2% to 3.0%, 0.6% to 1.1% and 3.0% to 4.4%. For the TG assay, total CVs at the laboratory were 0.2 to 1.9%. External quality assessment for the TG assay was performed by the Japan Association of Medical Technologists (JAMT) and the analytical performance of the TG assay has met the criteria of quality assessment in the JAMT.

2.3. Measurements of other risk factors

Plasma glucose concentrations were determined by the hexokinase method, and glycosylated hemoglobin (HbA1c) concentrations were determined by HPLC. Diabetes was defined as plasma glucose concentration being ≥7.0 mmol/l in fasting samples or ≥11.1 mmol/l in nonfasting samples, plasma HbA1c concentration being ≥6.5%, use of anti-diabetic agents or a combination of these.

Blood pressures were measured twice in the sitting position after urination and a 5-min rest by well-trained staff using an automatic device. Systolic blood pressure (SBP) and diastolic blood pressure (DBP) were each calculated as the mean of 2 measurements. Hypertension was defined as SBP being ≥140 mmHg, DBP being ≥90 mmHg or more, use of antihypertensive agents or a combination of these. Height in stockings and weight in light clothing were measured. Body mass index (BMI) was calculated as weight (kg) divided by the square of height (m).

Self-administered questionnaires for past history of stroke and myocardial infarction, medication, alcohol drinking and smoking status were used to collect individual information. To confirm whether participants had had prevalent stroke and myocardial infarction at the baseline survey, data from the Iwate Stroke Registry [26] and Northern Iwate Heart Disease Registry Consortium [27] were systematically reviewed. Smoking status was determined as current, past and never smoking by the questionnaire. Regular alcohol drinking was defined as drinking ≥5 days/week. Presence or absence of medication for dyslipidemia was determined by the answer of whether a participant had used any anti-hyperlipidemia agents.

2.4. Statistical analysis

All analyses, except for a logistic regression analysis, were separately performed in the fasting group and nonfasting group. Participants were also classified into 3 groups according to serum TG concentrations, of which cut-off points were based on the National Cholesterol Education Program Adult Treatment Panels III (NCEP-ATP III) guideline, i.e., normal: <1.69 mmol/l (150 mg/dl), moderate high: 1.69 to 2.26 mmol/l (150 to 199 mg/dl), and high: 2.26 to 4.51 mmol/l (200 to 399 mg/dl) [1]. We calculated the means and proportions of selected variables by TG group. Data for TG were expressed as geometric means. Except for TG, comparisons of selected variables between TG groups were performed using analysis of variance (ANOVA) for continuous variables and the χ^2 test for categorical variables. Concentrations of LDL-C (F) and LDL-C (D) were also compared using the paired t-test.

The correlation between LDL-C (F) and LDL-C (D) and the effect of TG concentrations on the difference in LDL-C by the 2 methods, which was calculated by subtracting LDL-C (F) from LDL-C (D) concentrations, were estimated using Pearson's correlation coefficients and linear regression analysis. To examine concordance of concentrations of

Table 1
Characteristics and serum lipid levels in fasting participants by TG groups.

	Total	TG group, mmol/L						P value[a]
		<1.69		1.69–2.26		2.26–4.51		
Number of fasting participants	3270	2906		224		140		
TG, mmol/L[b]	0.97 (1.6)	0.87 (1.4)		1.89 (1.1)		2.80 (1.2)		<0.001
Men, %	36.8	35.4		42.4		57.1		<0.001
Age, years	63.5 (9.3)	63.5 (9.4)		63.8 (8.9)		62.4 (9.4)		0.342
Body mass index, kg/m^2	24.0 (3.3)	23.8 (3.3)		25.1 (3.4)		25.6 (3.0)		<0.001
Hypertension, %	42.3	41.4		49.1		50.7		0.010
Diabetes, %	9.0	8.4		9.8		20.0		<0.001
Current smokers, %	11.2	10.4		14.3		22.1		<0.001
Regular drinkers, %	19.3	18.9		21.0		25.7		0.110
Serum lipids								
TC, mmol/L	5.31 (0.85)	5.27 (0.83)		5.53 (0.91)		5.73 (0.91)		<0.001
HDL-C, mmol/L	1.58 (0.39)	1.62 (0.39)		1.30 (0.30)		1.20 (0.29)		<0.001
non-HDL-C, mmol/L	3.73 (0.85)	3.65 (0.81)		4.23 (0.88)		4.53 (0.88)		<0.001
LDL-C (F), mmol/L	3.24 (0.77)	3.23 (0.76)		3.36 (0.87)		3.23 (0.88)		0.046
LDL-C (D), mmol/L	3.24 (0.76)	3.22 (0.75)		3.40 (0.83)		3.29 (0.83)		0.003
	$P=0.553$[c]	$P=0.232$[c]		$P=0.019$[c]		$P=0.033$[c]		

TG, triglyceride; TC, total cholesterol; LDL-C, low-density lipoprotein cholesterol; HDL-C, high-density lipoprotein cholesterol; LDL-C (F), LDL-C calculated by the Friedewald formula; LDL-C (D), LDL-C measured by the enzymatic homogeneous assay.
Data are expressed as means (standard deviations) for continuous variables and percentages for categorical variables.
[a] *P* values for comparisons of variables between TG groups by analysis of variance or the chi-squared test.
[b] Data for triglyceride are expressed as geometric means (geometric standard deviations).
[c] *P* values for comparisons between LDL-C (F) levels and LDL-C (D) levels by the paired t-test.

LDL-C (F) and LDL-C (D), participants were classified into four groups according to concentrations of LDL-C (F) or LDL-C (D) based on the LDL-C cut-off points recommended by the NCEP-ATP III guideline, i.e., <2.58 mmol/l (100 mg/dl), 2.58 to 3.35 mmol/l (100 to 129 mg/dl), 3.36 to 4.12 mmol/l (130 to 159 mg/dl), ≥4.13 mmol/l (160 mg/dl) [1]. Cross-tables among the NCEP groups of LDL-C (F) and LDL-C (D) were presented by TG groups.

Logistic regression analysis was performed for the all participants in the fasting and nonfasting groups. In the analysis, the dependent variable was discordance of the groups between LDL-C (F) and LDL-C (D) (coded as 1 for discordance and coded as 0 for concordance) and the independent variables were logarithm-transformed TG (ln TG), age, sex, BMI, hypertension (presence or absence), diabetes (presence or absence), current smokers (or not), regular drinkers (or not) and nonfasting state (or fasting state). In all analyses, 2-sided $P<0.05$ was considered to be statistically significant. The Statistical Package for Social Science (SPSS Japan Inc. ver. 15.0J, Tokyo, Japan) was used for all analyses.

3. Results

Table 1 shows characteristics of fasting participants by TG groups. There were significant differences between TG groups in all variables except for mean age and proportion of regular drinkers: that is, mean BMI and proportions of male participants, participants with hypertension, participants with diabetes and current smokers were higher in the higher TG group. Table 1 also shows fasting serum lipid profiles by TG groups. Mean concentrations of TC, HDL-C, non-HDL-C, LDL-C (F) and LDL-C (D) were significantly different between the TG groups. There was no significant difference between mean fasting concentrations of LDL-C (D) and LDL-C (F) (3.24 mmol/l and 3.24 mmol/l, respectively). In the normal TG group, there was also no significant difference between mean fasting concentrations of LDL-C (D) and LDL-C (F): mean concentrations of LDL-C (D) and LDL-C (F) were 3.22 mmol/l and 3.23 mmol/l, respectively. In the moderate high and high TG groups, mean fasting concentrations of LDL-C (D) were

Table 2
Characteristics and serum lipid levels in nonfasting participants by TG groups.

	Total	TG group, mmol/L						P value[a]
		<1.69		1.69–2.26		2.26–4.51		
Number of nonfasting participants	17,924	13,831		2307		1786		
TG, mmol/L[b]	1.16 (1.7)	0.95 (1.4)		1.92 (1.1)		2.86 (1.2)		<0.001
Men, %	34.3	32.8		36.7		42.8		<0.001
Age, years	62.1 (9.7)	62.1 (9.8)		62.4 (9.4)		61.7 (9.6)		0.071
Body mass index, kg/m^2	24.0 (3.3)	23.7 (3.2)		25.1 (3.2)		25.5 (3.1)		<0.001
Hypertension, %	40.6	38.3		47.9		49.2		<0.001
Diabetes, %	4.9	4.4		5.8		7.8		<0.001
Current smokers, %	12.7	11.6		14.5		18.5		<0.001
Regular drinkers, %	19.0	18.7		19.0		21.8		0.007
Serum lipids								
TC, mmo/L	5.15 (0.83)	5.07 (0.81)		5.36 (0.81)		5.50 (0.84)		<0.001
HDL-C, mmol/L	1.53 (0.38)	1.60 (0.38)		1.37 (0.31)		1.26 (0.29)		<0.001
Non-HDL-C, mmol/L	3.62 (0.82)	3.47 (0.77)		3.99 (0.77)		4.24 (0.81)		<0.001
LDL-C (F), mmol/L	3.01 (0.75)	3.01 (0.73)		3.11 (0.77)		2.91 (0.82)		<0.001
LDL-C (D), mmol/L	3.08 (0.74)	3.03 (0.73)		3.28 (0.73)		3.24 (0.76)		<0.001
	$P<0.001$[c]	$P<0.001$[c]		$P<0.001$[c]		$P<0.001$[c]		

TG, triglyceride; TC, total cholesterol; LDL-C, low-density lipoprotein cholesterol; HDL-C, high-density lipoprotein cholesterol; LDL-C (F), calculated by the Friedewald formula; LDL-C (D), LDL-C measured by the enzymatic homogeneous assay.
Data are expressed as means (standard deviations) for continuous variables and percentages for categorical variables.
[a] *P* values for comparisons of variables between TG groups by analysis of variance or the chi-squared test.
[b] Data for triglyceride are expressed as geometric means (geometric standard deviations).
[c] *P* values for comparisons between LDL-C (F) levels and LDL-C (D) levels by the paired t-test.

significantly higher than those of LDL-C (F): the differences were 0.04 mmol/l and 0.06 mmol/l, respectively.

Table 2 shows characteristics and serum lipid profiles of nonfasting participants by TG groups. The differences in variables and serum lipid profiles between TG groups in nonfasting participants were similar to those in fasting participants. However, there were significant differences between concentrations of LDL-C (D) and LDL-C (F): mean concentrations of LDL-C (D) and LDL-C (F) were 3.08 and 3.01 mmol/l. A difference between them was found even in the normal TG group: mean nonfasting concentrations of LDL-C (D) and LDL-C (F) were 3.03 mmol/l and 3.01 mmol/dl, although the difference was only 0.02 mmol/l. Moreover, mean nonfasting concentrations of LDL-C (D) were significantly higher than those of LDL-C (F) in the moderate and high TG groups: the differences were 0.17 mmol/l and 0.33 mmol/l, respectively.

Both in fasting and nonfasting samples, LDL-C (D) concentrations showed strong linear correlations with LDL-C (F) concentrations: Pearson's coefficient (r) for fasting samples and that for nonfasting samples was 0.971 and 0.955, respectively (both $P<0.001$) (Fig. 1). The effect of TG concentrations on the difference between concentrations of LDL-C (D) and LDL-C (F) differed between fasting and nonfasting samples. In fasting samples, the difference in LDL-C concentrations was positively related to TG concentrations (Pearson's correlation coefficient $r=0.157$, $P<0.001$) and it increased by 0.05 mmol/l with an increment of 1.00 mmol/l in TG concentration (Fig. 2A), whereas in nonfasting samples, the difference in LDL-C concentrations showed a relatively higher positive relation to TG concentrations compared with that in fasting samples (Pearson's correlation coefficient $r=0.523$, $P<0.001$) and increased by 0.17 mmol/l with an increment of 1.00 mmol/l in TG concentration (Fig. 2B).

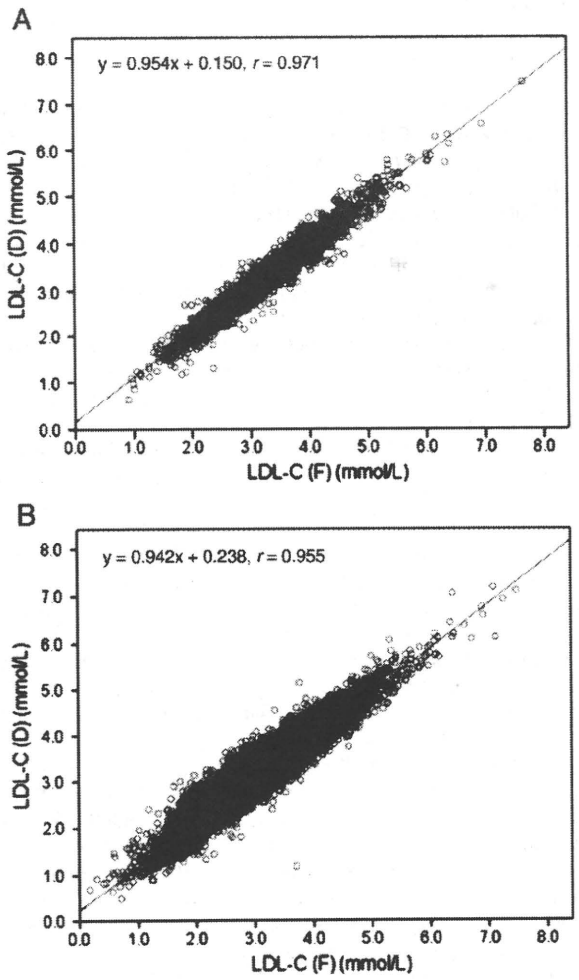

Fig. 1. Correlations between LDL-C (F) and LDL-C (D) in fasting participants (n = 3270) (A) and nonfasting participants (n = 17,294) (B). The solid lines represent regression lines.

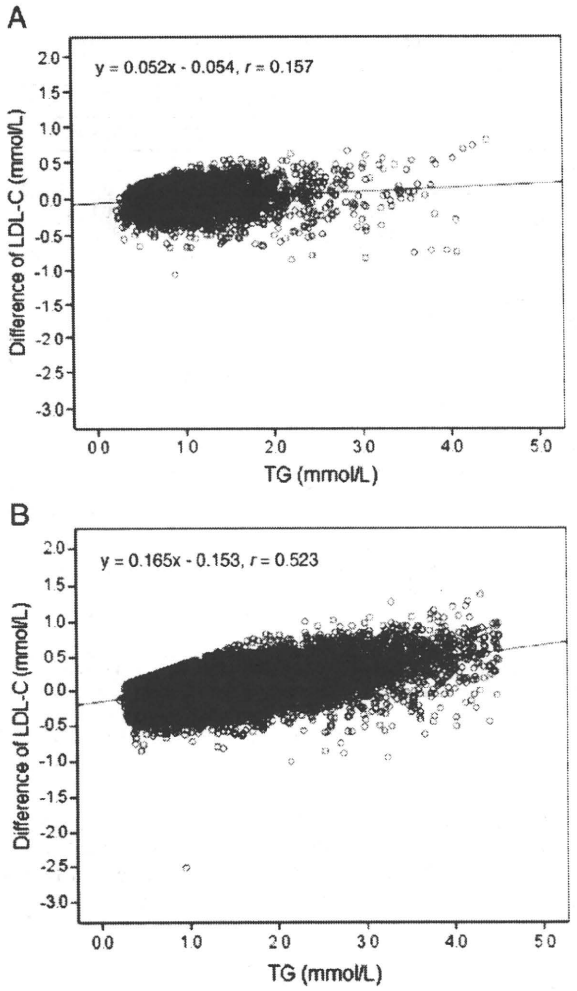

Fig. 2. Effect of increased TG concentrations on the difference in LDL-C concentrations between the homogeneous assay and the Friedewald formula in fasting participants (n = 3270) (A) and nonfasting participants (n = 17,294) (B). The difference in LDL-C, which is calculated by subtracting LDL-C concentrations by the Friedewald formula from those by the homogeneous assay, is plotted as a function of TG concentrations. The solid lines represent regression lines.

Table 3 shows concordance between fasting LDL-C (F) and LDL-C (D) for classifying participants into NCEP categories of risk. Overall, 2772 (84.8%) of the 3270 participants showed concordant results. A total of 497 fasting participants (15.2%) differed by one NCEP group. Of these, the proportions of fasting participants being classified into one upper group by LDL-C (D) concentrations compared with LDL-C (F) concentrations were 54.4% (228 of 420) in the normal TG group, 59.3% (19 of 32) in the moderate high TG group and 62.2% (28 of 45) in the high TG group.

Table 4 shows concordance between nonfasting LDL-C (F) and LDL-C (D) for classifying participants into NCEP categories of risk. Overall, 14,366 (80.1%) of 17,924 participants showed concordant results. A total of 3550 nonfasting participants (19.8%) differed by one NCEP group. Of these, the proportions of nonfasting participants being

Table 3
Concordance of NCEP groups between LDL-C (F) levels and LDL-C (D) levels in fasting participants.

			LDL-C (D), mmol/L			
			<2.59	2.60–3.36	3.36–4.13	4.13+
All fasting participants (n = 3270)						
LDL-C (F), mmol/L	<2.59	(n = 632)	86.6	13.4	0	0
	2.60–3.36	(n = 1273)	4.2	85.6	10.1	0
	3.36–4.13	(n = 976)	0.1	10.5	83.2	6.3
	4.13+	(n = 389)	0	0	17.0	83.0
Normal TG (<1.69 mmol/L) group (n = 2906)						
LDL-C (F), mmol/L	<2.59	(n = 571)	87.2	12.8	0	0
	2.60–3.36	(n = 1128)	4.1	86.9	9.0	0
	3.36–4.13	(n = 882)	0	10.3	83.7	6.0
	4.13+	(n = 325)	0	0	16.9	83.1
Moderate high TG (1.69–2.26 mmol/L) group (n = 224)						
LDL-C (F), mmol/L	<2.59	(n = 33)	87.9	12.1	0	0
	2.60–3.36	(n = 87)	2.3	82.8	14.9	0
	3.36–4.13	(n = 60)	1.7	8.3	86.7	3.3
	4.13+	(n = 44)	0	0	13.6	86.4
High TG (2.26–4.51 mmol/L) group (n = 140)						
LDL-C (F), mmol/L	<2.59	(n = 28)	71.4	28.6	0	0
	2.60–3.36	(n = 58)	10.3	65.5	24.1	0
	3.36–4.13	(n = 34)	0	17.6	64.7	17.6
	4.13+	(n = 20)	0	0	25.0	75.0

TG, triglyceride; LDL-C, low-density lipoprotein cholesterol; LDL-C (F), LDL-C calculated by the Friedewald formula; LDL-C (D), LDL-C measured by the enzymatic homogeneous assay.
Data are expressed as percentages of the number of participants being classified into each LDL-C (F) group.

classified into one upper group by LDL-C (D) concentrations compared with LDL-C (F) concentrations were 57.8% (1277 of 2210) in the normal TG group, 89.0% (541 of 608) in the moderate high TG group and 93.7% (686 of 732) in the high TG group.

Table 4
Concordance of NCEP groups between LDL-C (F) levels and LDL-C (D) levels in nonfasting participants.

			LDL-C (D), mmol/L			
			<2.59	2.60–3.36	3.36–4.13	4.13+
All nonfasting participants (n = 17,924)						
LDL-C (F), mmol/L	<2.59	(n = 5134)	79.2	20.7	0.1	0
	2.60–3.36	(n = 7294)	5.4	79.8	14.7	0
	3.36–4.13	(n = 4241)	0	10.6	80.8	8.7
	4.13+	(n = 1255)	0	0	16.0	84.0
Normal TG (<1.69 mmol/L) group (n = 13,831)						
LDL-C (F), mmol/L	<2.59	(n = 3959)	86.0	14.0	0	0
	2.60–3.36	(n = 5698)	6.5	84.2	9.2	0
	3.36–4.13	(n = 3240)	0	12.2	81.7	6.0
	4.13+	(n = 934)	0	0	17.6	82.4
Moderate high TG (1.69–2.26 mmol/L) group (n = 2307)						
LDL-C (F), mmol/L	<2.59	(n = 556)	64.2	35.8	0	0
	2.60–3.36	(n = 935)	1.3	69.9	28.8	0
	3.36–4.13	(n = 609)	0	5.4	82.6	12.0
	4.13+	(n = 207)	0	0	10.6	89.4
High TG (2.26–4.51 mmol/L) group (n = 1786)						
LDL-C (F), mmol/L	<2.59	(n = 619)	49.3	49.9	0.8	0
	2.60–3.36	(n = 661)	1.8	55.8	42.1	0.3
	3.36–4.13	(n = 392)	0	4.8	69.9	25.3
	4.13+	(n = 114)	0	0	13.2	86.8

TG, triglyceride; LDL-C, low-density lipoprotein cholesterol; LDL-C (F), LDL-C calculated by the Friedewald formula; LDL-C (D), LDL-C measured by the enzymatic homogeneous assay.
Data are expressed as percentages of the number of participants being classified into each LDL-C (F) group.

Table 5
Odds ratios for discordance of NCEP groups between LDL-C (F) and LDL-C (D) for each factor.

	OR	(95% CI)	*P* value
ln TG (per 1-ln TG increase)	2.44	(2.26–2.63)	<0.001
Sex (men/women)	1.01	(0.92–1.11)	0.856
Age (per 1-year increase)	1.00	(0.99–1.00)	0.052
Body mass index (per 1-kg/m^2 increase)	1.00	(0.99–1.01)	0.663
Hypertension (presence/absence)	1.01	(0.93–1.09)	0.846
Diabetes (presence/absence)	1.21	(1.05–1.40)	0.009
Current smoking (yes/no)	0.96	(0.85–1.08)	0.473
Regular drinking (yes/no)	0.92	(0.82–1.02)	0.108
Nonfasting state (/fasting state)	1.18	(1.06–1.31)	0.002

LDL-C, low-density lipoprotein cholesterol; LDL-C (F), LDL-C calculated by the Friedewald formula; LDL-C (D), LDL-C measured by the enzymatic homogeneous assay; OR, odds ratio; CI, confidence interval; ln TG, logarithm-transformed triglyceride. The OR was adjusted for ln TG, sex, age, body mass index, hypertension, diabetes, current smoking, regular drinking and nonfasting state.

For all participants in the fasting and nonfasting groups, the logistic regression model revealed that the discordance of NCEP groups between LDL-C (F) and LDL-C (D) was associated with higher TG concentrations: the odds ratio (OR) (95% confidence interval (CI)) was 2.44 (2.26–2.63) with an increment of 1-ln TG. In addition, the presence of diabetes and nonfasting state was associated with the discordance between the two methods: ORs (95% CIs) were 1.21 (1.05–1.40) for the presence of diabetes and 1.18 (1.06–1.31) for the nonfasting state (Table 5).

4. Discussion

We demonstrated that LDL-C (D) concentrations had a significant correlation with LDL-C (F) concentrations and that NCEP categories of LDL-C (D) were highly coincident with those of LDL-C (F) in fasting samples. In addition, even in nonfasting samples, the correlation coefficient between LDL-C (D) and LDL-C (F) concentrations was more than 0.9 and the concordance rate of NCEP categories between the two LDL-C concentrations was approximately 80%. However, the discordance was increased in samples with higher TG concentrations, particularly in nonfasting samples.

Our findings in fasting samples are similar to results of previous studies in Western countries [28–30] and other countries [31–33] showing a strong correlation between concentrations of LDL-C (D) and LDL-C (F). Two studies have shown the concordance rate of calculated LDL-C and directly measured LDL-C for classifying participants into NCEP categories [29,30]. One of those studies used data for LDL-C concentrations measured by an immunoseparation method in 661 primary care patients who had TG concentrations less than 4.52 mmol/l (mean, 1.66 mmol/l) and who were not receiving medication for hyperlipidemia. The other study used data for LDL-C concentrations measured by an enzymatic homogeneous method in 19,777 female healthcare professionals who had TG concentrations <4.52 mmol/l (mean, 1.53 mmol/l) and no history of CVD or cancer. The concordance rates were 48.1% in the former study [29] and 79.3% in the latter study [30]. The concordance rate in the present study (84.8%) was similar to that in the latter study.

On the other hand, we showed that fasting LDL-C (D) concentrations were significantly higher than fasting LDL-C (F) concentrations when TG concentrations were ≥1.69 mmol/l, although the difference between the two LDL-C concentrations was small. Most previous studies [28,29,31–33], except for one study [30], have demonstrated that LDL-C concentrations determined by direct methods tend to be higher than those calculated by the Friedewald formula, especially in subjects with higher TG concentrations.

The Friedewald formula is known to underestimate LDL-C concentrations compared with those measured by β-quantification even in fasting samples with TG concentrations being <4.52 mmol/l [13–15].

The bias increases with increasing TG concentrations, starting at moderate high TG concentrations (1.5 or 2.0 mmol/l) [13,14]. Miller et al. simultaneously compared the Friedewald formula and the enzymatic homogeneous assay, which was the same one as that used in the present study, with β-quantification [12]. They showed that the homogeneous assay had less variability in LDL-C concentrations than did the Friedewald formula in TG concentrations between 3.39 and 6.77 mmol/l (300 and 600 mg/dl) [12]. Therefore, the reason for the higher LDL-C concentrations obtained by the direct assay in fasting samples with TG concentrations being ≥1.69 mmol/l may be due to underestimation of LDL-C concentrations by the Friedewald formula.

A recent cohort study suggested that epidemiological studies could use LDL-C concentrations calculated by the Friedewald formula in participants with nonfasting samples to assess the association of LDL-C with CVD risk [20]. However, some studies have also shown that LDL-C concentrations calculated by the Friedewald formula significantly decrease at the postprandial state [16–18] and that the LDL-C concentrations calculated by the Friedewald formula are also significantly lower than those measured by β-quantification in postprandial samples among the same individuals [16]. On the other hand, there was no significant difference in LDL-C concentrations measured by the same homogeneous assay as that used in our study between paired fasting and nonfasting samples from the same individuals [10,11]. Miller et al. showed that postprandial changes in LDL-C concentrations measured by the assay used in our study were similar to those measured by β-quantification, although LDL-C concentrations measured by the assay in postprandial samples were significantly lower than those in fasting samples [12]. Indeed, we also showed that nonfasting LDL-C concentrations calculated by the Friedewald formula were significantly lower than those measured by the homogeneous assay, particularly in samples with TG being 1.69 mmol/l or greater. The results suggest that the bias between the Friedewald formula and the direct homogeneous assay observed in our study is comparable to the bias between the Friedewald formula and β-quantification in the literature.

We also demonstrated that the discordance of NCEP categories between LDL-C (F) and LDL-C (D) was associated with diabetes as well as higher TG concentrations and nonfasting state. Some studies showed poor validity of the Friedewald formula in diabetic patients [34,35], whereas the homogeneous assay used in our study did not seem to be compromised in diabetic patients [36]. The above-mentioned findings indicate the possibility of less variability of this homogeneous assay than that of the Friedewald formula in nonfasting samples.

The present study has several limitations. First, most participants were in a nonfasting state. However, precisely because all participants were not at a fasting state, we believe that it was significant to perform a direct measurement of LDL-C concentrations. Second, we did not use β-quantification as the standard reference method. Thus, it is not clear whether the homogeneous assay overestimated the LDL-C concentration or whether the Friedewald formula underestimated the LDL-C concentration. Third, our subjects were an apparently healthy population; thus, it is unclear if our results would be applicable to diseased populations, particularly patients with hypertriglycemia or CVD. Finally, it is possible that our results may not be directly applicable to those obtained from other homogeneous assays because the present results were obtained from the direct assay by Daiichi Chemicals (currently Sekisui Medical).

In conclusion, we demonstrated a strong correlation between LDL-C concentrations measured by the direct homogeneous assay and those calculated by the Friedewald formula and high concordance rates of NCEP groups between the two LDL-C concentrations in fasting samples; however, it should be kept in mind that LDL-C concentrations measured by the direct homogeneous assay tend to be slightly higher than calculated LDL-C concentrations when TG concentrations are ≥1.69 mmol/l. We also showed less variability of the direct homogeneous assay than that of the Friedewald formula in large numbers of nonfasting samples. The bias between the Friedewald formula and the direct homogeneous assay observed in our study was comparable to the bias between the Friedewald formula and β-quantification in the literature. The findings suggest that the direct assay for LDL-C measurement can be used in epidemiological studies on the association of LDL-C with risk for CVD both in fasting and nonfasting samples. Future longitudinal studies are needed to clarify the utility of direct nonfasting LDL-C measurements as a predictor of CVD events.

Acknowledgments

This study was supported by grants from the Japan Arteriosclerosis Prevention Fund and the Ministry of Health, Labour and Welfare of Japan (H17-Choju-025 and H19-Choju-030). We would like to thank the staff of the Iwate Health Service Association and the staff in all municipalities (Iwate Prefecture, Ninohe City, Ichinohe Town, Karumai Town, Kunohe Village, Yamada Town, Kawai Village, Miyako City, Niisato Village, Taro Town, Iwaizumi Town, Tanohata Village, Kuji City, Yamagata Village, Fudai Village, Ohno Village, Noda Village, and Taneichi Town).

References

[1] National Cholesterol Education Program (NCEP) Expert Panel on Detection, Evaluation, and Treatment of High Blood Cholesterol in Adults (Adult Treatment Panel III). Third report of the National Cholesterol Education Program (NCEP) Expert Panel on Detection, Evaluation, and Treatment of High Blood Cholesterol in Adults (Adult Treatment Panel III) final report. Circulation 2002;106:3143–421.
[2] Teramoto T, Sasaki J, Ueshima H, et al. Executive summary of Japan Atherosclerosis Society (JAS) guideline for diagnosis and prevention of atherosclerotic cardiovascular diseases for Japanese. J Atheroscler Thromb 2007;14:45–50.
[3] Friedewald WT, Levy RI, Fredrickson DS. Estimation of the concentration of low-density lipoprotein cholesterol in plasma, without use of the preparative ultracentrifuge. Clin Chem 1972;18:499–502.
[4] Wilson PW, D'Agostino RB, Levy D, Belanger AM, Silbershatz H, Kannel WB. Prediction of coronary heart disease using risk factor categories. Circulation 1998;97:1837–47.
[5] Sharrett AR, Ballantyne CM, Coady SA, et al. Coronary heart disease prediction from lipoprotein cholesterol concentrations, triglycerides, lipoprotein(a), apolipoproteins A-I and B, and HDL density subfractions: the Atherosclerosis Risk in Communities (ARIC) study. Circulation 2001;104:1108–13.
[6] Okamura T, Kokubo Y, Watanabe M, et al. Low-density lipoprotein cholesterol and non-high-density lipoprotein cholesterol and the incidence of cardiovascular disease in an urban Japanese cohort study: the Suita study. Atherosclerosis 2009;203:587–92.
[7] Maruyama K, Hirobe K, Noda H, et al. Associations between blood lipid profiles and risk of myocardial infarction among Japanese male workers: 3 M study. J Atheroscler Thromb 2009;16:714–21.
[8] Miller WG, Myers GL, Sakurabayashi I, et al. Seven direct methods for measuring HDL and LDL cholesterol compared with ultracentrifugation reference measurement procedures. Clin Chem 2010;56:977–86.
[9] Nauck M, Warnick GR, Rifai N. Methods for measurement of LDL-cholesterol: a critical assessment of direct measurement by homogeneous assays versus calculation. Clin Chem 2002;48:236–54.
[10] Rifai N, Iannotti E, DeAngelis K, Law T. Analytical and clinical performance of a homogeneous enzymatic LDL-cholesterol assay compared with the ultracentrifugation-dextran sulfate-Mg^{2+} method. Clin Chem 1998;44:1242–50.
[11] Yu HH, Markowitz R, De Ferranti SD, et al. Direct measurement of LDL-C in children: performance of two surfactant-based methods in a general pediatric population. Clin Biochem 2000;33:89–95.
[12] Miller WG, Waymack PP, Anderson FP, Ethridge SF, Jayne EC. Performance of four homogeneous direct methods for LDL-cholesterol. Clin Chem 2002;48:489–98.
[13] DeLong DM, DeLong ER, Wood PD, Lippel K, Rifkind BM. A comparison of methods for the estimation of plasma low- and very low-density lipoprotein cholesterol. The lipid research clinics prevalence study. JAMA 1986;256:2372–7.
[14] Marniemi J, Maki J, Maatela J, Jarvisalo J, Impivaara O. Poor applicability of the Friedewald formula in the assessment of serum LDL cholesterol for clinical purposes. Clin Biochem 1995;28:285–9.
[15] Tremblay AJ, Morrissette H, Gagne JM, Bergeron J, Gagne C, Couture P. Validation of the Friedewald formula for the determination of low-density lipoprotein cholesterol compared with beta-quantification in a large population. Clin Biochem 2004;37:785–90.
[16] Cohn JS, McNamara JR, Schaefer EJ. Lipoprotein cholesterol concentrations in the plasma of human subjects as measured in the fed and fasted states. Clin Chem 1988;34:2456–9.
[17] Rifai N, Merrill JR, Holly RG. Postprandial effect of a high fat meal on plasma lipid, lipoprotein cholesterol and apolipoprotein measurements. Ann Clin Biochem 1990;27(Pt 5):489–93.
[18] Wilder LB, Bachorik PS, Finney CA, Moy TF, Becker DM. The effect of fasting status on the determination of low-density and high-density lipoprotein cholesterol. Am J Med 1995;99:374–7.

[19] Noda H, Iso H, Irie F, et al. Low-density lipoprotein cholesterol concentrations and death due to intraparenchymal hemorrhage: the Ibaraki Prefectural Health Study. Circulation 2009;119:2136–45.
[20] Noda H, Iso H, Irie F, Sairenchi T, Ohtaka E, Ohta H. Gender difference of association between LDL cholesterol concentrations and mortality from coronary heart disease amongst Japanese: the Ibaraki Prefectural Health Study. J Intern Med 2010;267:576–87.
[21] Langsted A, Freiberg JJ, Nordestgaard BG. Fasting and nonfasting lipid concentrations: influence of normal food intake on lipids, lipoproteins, apolipoproteins, and cardiovascular risk prediction. Circulation 2008;118:2047–56.
[22] Ohsawa M, Itai K, Tanno K, et al. Cardiovascular risk factors in the Japanese northeastern rural population. Int J Cardiol 2009;137:226–35.
[23] Ohsawa M, Itai K, Onoda T, et al. Dietary intake of n-3 polyunsaturated fatty acids is inversely associated with CRP concentrations, especially among male smokers. Atherosclerosis 2008;201:184–91.
[24] Makita S, Nakamura M, Satoh K, et al. Serum C-reactive protein concentrations can be used to predict future ischemic stroke and mortality in Japanese men from the general population. Atherosclerosis 2009;204:234–8.
[25] Nakamura M, Sato S, Shimamoto T. Improvement in Japanese clinical laboratory measurements of total cholesterol and HDL-cholesterol by the US Cholesterol Reference Method Laboratory Network. J Atheroscler Thromb 2003;10:145–53.
[26] Omama S, Yoshida Y, Ogawa A, Onoda T, Okayama A. Differences in circadian variation of cerebral infarction, intracerebral haemorrhage and subarachnoid haemorrhage by situation at onset. J Neurol Neurosurg Psychiatry 2006;77:1345–9.
[27] Ogawa M, Tanaka F, Onoda T, et al. A community based epidemiological and clinical study of hospitalization of patients with congestive heart failure in Northern Iwate, Japan. Circ J 2007;71:455–9.
[28] Faas FH, Earleywine A, Smith G, Simmons DL. How should low-density lipoprotein cholesterol concentration be determined? J Fam Pract 2002;51:972–5.
[29] Tighe DA, Ockene IS, Reed G, Nicolosi R. Calculated low density lipoprotein cholesterol concentrations frequently underestimate directly measured low density lipoprotein cholesterol determinations in patients with serum triglyceride concentrations ≤4.52 mmol/l: an analysis comparing the LipiDirect magnetic LDL assay with the Friedewald calculation. Clin Chim Acta 2006;365:236–42.
[30] Mora S, Rifai N, Buring JE, Ridker PM. Comparison of LDL cholesterol concentrations by Friedewald calculation and direct measurement in relation to cardiovascular events in 27,331 women. Clin Chem 2009;55:888–94.
[31] Can M, Acikgoz S, Mungan G, et al. Is direct method of low density lipoprotein cholesterol measurement appropriate for targeting lipid lowering therapy? Int J Cardiol 2010;142:105–7.
[32] Cordova CM, Schneider CR, Juttel ID, Cordova MM. Comparison of LDL-cholesterol direct measurement with the estimate using the Friedewald formula in a sample of 10, 664 patients. Arq Bras Cardiol 2004;83(482–487):476–81.
[33] Jun KR, Park HI, Chun S, Park H, Min WK. Effects of total cholesterol and triglyceride on the percentage difference between the low-density lipoprotein cholesterol concentration measured directly and calculated using the Friedewald formula. Clin Chem Lab Med 2008;46:371–5.
[34] Branchi A, Rovellini A, Torri A, Sommariva D. Accuracy of calculated serum low-density lipoprotein cholesterol for the assessment of coronary heart disease risk in NIDDM patients. Diab Care 1998;21:1397–402.
[35] Hirany S, Li D, Jialal I. A more valid measurement of low-density lipoprotein cholesterol in diabetic patients. Am J Med 1997;102:48–53.
[36] Ragland BD, Konrad RJ, Chaffin C, Robinson CA, Hardy RW. Evaluation of a homogeneous direct LDL-cholesterol assay in diabetic patients: effect of glycemic control. Clin Chem 2000;46:1848–51.

Neurogenetics (2011) 12:25–31
DOI 10.1007/s10048-010-0260-7

ORIGINAL ARTICLE

Partial *SPAST* and *DPY30* deletions in a Japanese spastic paraplegia type 4 family

Shiroh Miura · Hiroki Shibata · Hiroshi Kida · Kazuhito Noda · Takayuki Toyama · Naoka Iwasaki · Akiko Iwaki · Mitsuyoshi Ayabe · Hisamichi Aizawa · Takayuki Taniwaki · Yasuyuki Fukumaki

Received: 9 July 2010 / Accepted: 1 September 2010 / Published online: 22 September 2010

Abstract Spastic paraplegia type 4 (SPG4) is the most common autosomal dominant hereditary SPG caused by mutations in the *SPAST* gene. We studied the four-generation pedigree of a Japanese family with autosomal dominant hereditary SPG both clinically and genetically. Twelve available family members (ten affected; two unaffected) and two spouses were enrolled in the study. The clinical features were hyperreflexia in all four limbs, spasticity of the lower extremities, impaired vibration sense, mild cognitive impairment confirmed by the Wechsler Adult Intelligence Scale—Third Edition, and peripheral neuropathy confirmed by neurophysiological examinations. All four female patients experienced miscarriages. The cerebrospinal fluid tau levels were mildly increased in two of three patients examined. Linkage analyses revealed the highest logarithm of odds score of 2.64 at 2p23-p21 where the *SPAST* gene is located. Mutation scanning of the entire exonic regions of the *SPAST* gene by direct sequencing revealed no mutations. Exonic copy number analysis by real-time quantitative polymerase chain reaction revealed heterozygous deletion of exons 1 to 4 of the *SPAST* gene. Breakpoint analysis showed that the centromeric breakpoint was located within intron 4 of *SPAST* while the telomeric breakpoint was located within intron 3 of the neighboring *DPY30* gene, causing a deletion of approximately 70 kb ranging from exons 1 to 3 of *DPY30* to exons 1 to 4 of *SPAST*. To our knowledge, this is the first report of SPG4 associated with partial deletions of both the *SPAST* and *DPY30* genes. The partial heterozygous deletion of *DPY30* could modify the phenotypic expression of SPG4 patients with this pedigree.

Keywords Deletion · Hereditary spastic paraplegia type 4 (SPG4) · Neuropathy · Miscarriage · *SPAST* · *DPY30* · tau

S. Miura (✉) · H. Kida · K. Noda · T. Toyama · N. Iwasaki · M. Ayabe · H. Aizawa · T. Taniwaki
Division of Respirology, Neurology and Rheumatology, Department of Medicine, Kurume University School of Medicine, 67 Asahi-machi, Kurume, Fukuoka 830-0011, Japan
e-mail: shiroh46@med.kurume-u.ac.jp

H. Shibata · A. Iwaki · Y. Fukumaki
Division of Human Molecular Genetics, Research Center for Genetic Information, Medical Institute of Bioregulation, Kyushu University, 3-1-1 Maidashi, Higashi-ku, Fukuoka 812-8582, Japan

Introduction

Hereditary spastic paraplegia (SPG) comprises a group of clinically and genetically heterogeneous inherited disorders characterized by progressive lower limb spasticity and weakness. To date, 17 types of autosomal dominant SPG have been assigned to distinct loci of the human genome, and specific mutations for ten of the 17 types of autosomal dominant SPG have been identified.

SPG4 is the most common form of autosomal dominant hereditary SPG caused by mutations in the *SPAST* gene located at 2p22-p21. *SPAST* encodes a protein with a microtubule-interacting and endosomal trafficking domain at the N terminus associated with binding of microtubules and a member of the ATPase associated with various cellular activities (AAA) protein family at the C terminus associated with microtubule severing [1–6]. Many different mutations associated with SPG4, including missense, nonsense, or splice-site mutations; small insertions or deletions; and large duplications or deletions, have been identified in *SPAST* [2, 7–26]. There are some reports of

SPAST exon 1 deletions [7–11], but no reports of entire deletion of the first exon including the 5′-untranslated region (5′-UTR) of *SPAST* because most previous studies did not investigate the 5′ extent. Here, we report the first familial cases of SPG4 with deletions of exons 1 to 4 including the entire 5′-UTR of *SPAST*. Moreover, we identified a deletion involving the *DPY30* gene in these cases.

Subjects and methods

Subjects We studied a four-generation Japanese pedigree with SPG4 originating from Miyazaki prefecture, a southern province of Japan. Figure 1 shows an extract from this pedigree. After informed consent was obtained, 12 available family members and two spouses underwent a neurological examination and gave blood samples in 2007. Neuroimaging studies, neurophysiological studies, cerebrospinal fluid (CSF) examination, and cognitive tests were performed in three affected individuals (III-8, IV-1, and IV-2). This study was approved by the Ethics Committees of Kurume University School of Medicine and Kyushu University Faculty of Medicine.

Genotype analysis We scanned chromosomes 2 using 26 fluorescently labeled microsatellite markers that were chosen from the ABI PRISM Linkage Mapping Set Version 2.5 (Applied Biosystems, Foster City, CA, USA) and the NCBI database (Build 36.2), such that the markers were evenly spaced with average intervals of 13 Mb. Polymerase chain reaction (PCR) amplifications were performed as recommended by the supplier (Applied Biosystems) or using three-step methods. The amplified fragments with internal-size standards were resolved using an automated ABI PRISM 3100 DNA sequencer and analyzed using GENESCAN version 3.7 software (Applied Biosystems).

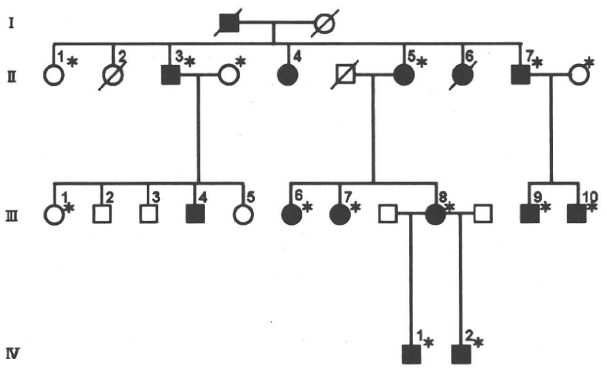

Fig. 1 Family pedigree (with partial omissions for protection against identification of other family members). *Squares* males, *circles* females, *solid symbols* affected individuals, *open symbols* unaffected individuals. Deceased individuals are indicated by *diagonal lines*. Family members used for the linkage analysis are marked by *asterisks*

Linkage analysis Multipoint logarithm of odds (LOD) scores were calculated using the GENEHUNTER program (Version 2.1_v2 beta) under the assumptions of autosomal dominant inheritance, disease frequency of one per 100,000, penetrance of 0.90, and equal frequencies of all alleles of each marker.

Mutation analysis We designed primers to examine the entire exonic sequences of *SPAST* (MIM 604277) by direct sequencing. We divided the large exons into several overlapping PCR fragments. We sequenced both strands of the PCR products using a BigDye Terminator v3.1 Sequencing Standard Kit (Applied Biosystems) and the automated ABI PRISM 3100 DNA sequencer.

Real-time quantitative PCR Six DNA samples obtained from three of the patients (III-8, IV-1, and IV-2) and three members of a family with hereditary motor and sensory neuropathy with proximal dominancy as controls [27] were used for copy number analyses. The PCR amplifications were performed in a total volume of 20 μl, containing 5 ng of genomic DNA, 2× Power SYBR Green PCR Master Mix (Applied Biosystems), and 250 nM of the forward and reverse primers. The real-time PCR amplifications were performed in an ABI PRISM 7000 Sequence Detection System (Applied Biosystems). To normalize the amount of each target DNA, the *RNase P* gene was amplified in a separate reaction well. The reactions were performed in a total volume of 20 μl, containing genomic DNA, 2× TaqMan Universal PCR Master Mix (Applied Biosystems), and 1 μl of TaqMan RNase P control reagents (VIC; Applied Biosystems). Each reaction was performed in triplicate.

Isolation and sequence analysis of the junction fragment Several forward and reverse primers were prepared within intron 3 of *DPY30* and intron 4 of *SPAST*, respectively. PCR amplifications were carried out using genomic DNA from patient III-8 with a pair of primers and a BigDye Terminator v3.1 Sequencing Standard Kit (Applied Biosystems), and the DNA sequences were determined in the automated ABI PRISM 3100 DNA sequencer.

Deletion-specific PCR For efficient detection of the deletion in the members of this family, genomic DNA (5 ng) was subjected to PCR amplification in a total volume of 10 μl, containing 500 nM each of the primers DPY30in3.13F (5′-CACATGCTGACACCCAGGCT-3′), SPASTin4.33R (5′-GGCAACAGAGCAACTCAGTCT-3′), and DPY30in3.1R (5′-CGATCTTTTGGGATGTTGCT-3′).